Molecular Phylogenetics and Evolution 138 (2019) 89–101

Contents lists available at ScienceDirect

Molecular Phylogenetics and Evolution

journal homepage: www.elsevier.com/locate/ympev

Coalescent-based species delimitation in the sand lizards of the *Liolaemus wiegmannii* complex (Squamata: Liolaemidae)

Joaquín Villamil[a,*], Luciano J. Avila[b], Mariana Morando[b], Jack W. Sites Jr.[c], Adam D. Leaché[d], Raúl Maneyro[a], Arley Camargo[e]

[a] Laboratorio de Sistemática e Historia Natural de Vertebrados, Instituto de Ecología y Ciencias Ambientales, Facultad de Ciencias, UdelaR, Iguá 4225, Montevideo, Uruguay
[b] Instituto Patagónico para el Estudio de los Ecosistemas Continentales (IPEEC, CENPAT-CONICET), Bv. Brown 2915, U9120ACD Puerto Madryn, Chubut, Argentina
[c] Department of Biology and Bean Life Science Museum, Brigham Young University, Provo, UT 84602, USA
[d] Department of Biology and Burke Museum of Natural History and Culture, University of Washington, Box 351800, Seattle, WA 98195-1800, USA
[e] Centro Universitario de Rivera, Universidad de la República, Ituzaingó 667, Rivera 40000, Uruguay

ARTICLE INFO

Keywords:
ddRADseq
Bayes factor species delimitation
SNPs
Species tree

ABSTRACT

Coalescent-based algorithms coupled with the access to genome-wide data have become powerful tools for assessing questions on recent or rapid diversification, as well as delineating species boundaries in the absence of reciprocal monophyly. In southern South America, the diversification of *Liolaemus* lizards during the Pleistocene is well documented and has been attributed to the climatic changes that characterized this recent period of time. Past climatic changes had harsh effects at extreme latitudes, including Patagonia, but habitat changes at intermediate latitudes of South America have also been recorded, including expansion of sand fields over northern Patagonia and Pampas). In this work, we apply a coalescent-based approach to study the diversification of the *Liolaemus wiegmannii* species complex, a morphologically conservative clade that inhabits sandy soils across northwest and south-central Argentina, and the south shores of Uruguay. Using four standard sequence markers (mitochondrial DNA and three nuclear loci) along with ddRADseq data we inferred species limits and a time-calibrated species tree for the *L. wiegmannii* complex in order to evaluate the influence of Quaternary sand expansion/retraction cycles on diversification. We also evaluated the evolutionary independence of the recently described *L. gardeli* and inferred its phylogenetic position relative to *L. wiegmannii*. We find strong evidence for six allopatric candidate species within *L. wiegmannii,* which diversified during the Pleistocene. The Great Patagonian Glaciation (~1 million years before present) likely split the species complex into two main groups: one composed of lineages associated with sub-Andean sedimentary formations, and the other mostly related to sand fields in the Pampas and northern Patagonia. We hypothesize that early speciation within *L. wiegmannii* was influenced by the expansion of sand dunes throughout central Argentina and Pampas. Finally, *L. gardeli* is supported as a distinct lineage nested within the *L. wiegmannii* complex.

1. Introduction

Species are the fundamental units in biology, and consequently, species delimitation is a central issue in systematics. Accurately estimating species limits represents a step towards the stabilization of alpha taxonomy, upon which many biogeographical, evolutionary and ecological studies rely. Ultimately, an adequate understanding of species diversity has important implications for conservation initiatives and their adequate funding (Agapow et al., 2004; Fujita et al., 2012). Unresolved species complexes are still relatively common in the Tree of Life, and this problem seems particularly common in species-rich groups that often show conservative morphology and/or have diverged recently (Bickford et al., 2007; Pfenninger and Schwenk, 2007; Pante et al., 2015a; Struck et al., 2018). In some cases, the use of morphology or gene trees alone has led to oversplitting of populations that might not represent distinct species, leading to taxonomic inflation (Fujita et al., 2011; but also see Bauer et al., 2011). Despite these limitations, the recent development of coalescent-based species delimitation methods has provided promising tools for testing hypotheses of species boundaries, especially for morphologically conserved groups and for populations/species that diverged recently (Fujita et al., 2012).

The genus *Liolaemus* is one of the most species-rich lizard genera in

* Corresponding author.
E-mail address: joakorep@gmail.com (J. Villamil).

https://doi.org/10.1016/j.ympev.2019.05.024
Received 8 March 2019; Received in revised form 21 May 2019; Accepted 21 May 2019
Available online 22 May 2019
1055-7903/

the world and contains around 260 recognized species widely distributed across southern South America (Pincheira-Donoso et al., 2008; Lobo et al., 2010; Breitman et al., 2011a; Avila et al., 2013; Uetz, 2019). In the last two decades, increased sampling efforts in unexplored areas coupled with the use of molecular markers have revealed multiple examples of widely distributed "species" characterized by high levels of cryptic diversity (Olave et al., 2017 and references therein). Many new species of *Liolaemus* have been described in the last ten years due to the resolution of species complexes (*e.g.,* Breitman et al., 2011b, 2011c; Martinez et al., 2011; Avila et al., 2017), or the discovery of new populations (*e.g.* Avila et al., 2009, 2012, 2015; Troncoso-Palacios et al., 2016; Verrastro et al., 2017; Vega et al., 2018). As the result of a complex evolutionary history, *Liolaemus* is now interpreted to include two major clades or subgenera (*Liolaemus sensu stricto* and *Eulaemus*), each containing several sections, series, species groups, and complexes (Schulte et al., 2000; Abdala and Quinteros, 2014; Olave et al., 2014). Within the *L. montanus* section of *Eulaemus,* morphological, behavioral and molecular studies have resolved a clade of arenicolous lizards known as the *Liolaemus wiegmannii* group (Etheridge, 1995, 2000; Schulte et al., 2000; Avila et al., 2006, 2009; Pincheira-Donoso et al., 2008; Olave et al., 2014; Verrastro et al., 2017), and we focus on part of this clade here.

Liolaemus wiegmannii (Duméril and Bibron 1837) is one of twelve species belonging to the *L. wiegmannii* group; it is distributed throughout several provinces of Argentina (Rio Negro, La Pampa, Buenos Aires, San Luis, Mendoza, Córdoba, Entre Ríos, Catamarca, San Juan, Tucumán, Salta, and Jujuy, including also a historical record from Santa Fé), and along the southwest, southern, and eastern shores of Uruguay (Etheridge, 2000; Avila et al., 2013) (Fig. 1i). Across this extensive range, the species occupies a great variety of sandy habitats. For instance, in Mendoza and some localities in Rio Negro and La Pampa, *L. wiegmannii* occurs in sandy soils and small dunes surrounded by Monte Desert vegetation (at sea level or below 500 m of altitude). Populations in other localities in La Pampa, San Luis, the south of Córdoba, Entre Ríos and inland Buenos Aires, live in Pampean sand dunes, while coastal populations in Buenos Aires Province and Uruguay inhabit vegetated coastal dunes. In the surroundings of the Sierras de Córdoba, *L. wiegmannii* is found in open areas of Chaco Serrano environments. Finally, in Catamarca, Tucuman, Salta, and Jujuy Provinces, the species is observed in sedimentary formations of sub-Andean mountain ranges where altitudes can reach ~2000 m above sea level (masl) (Etheridge, 2000; this study). Several authors have pointed out that *L. wiegmannii* is probably a species complex, and that some disjunct populations may represent independent evolutionary lineages (Etheridge, 2000; Avila, 2003; Avila et al., 2006, 2009). In fact, Avila et al. (2009) inferred a phylogeny of the *L. wiegmannii* group that resolved four lineages: *L. wiegmannii, L. wiegmannii*-Uruguay, *L. wiegmannii*-Mendoza, and *L. wiegmannii*-Catamarca. However, this study did not include either the northernmost known populations (*i.e.,* Tucumán, Salta, and Jujuy), or *L. gardeli* (Verrastro et al., 2017), a recently described species from isolated sand dunes in central Uruguay, which is a nested lineage within the *L. wiegmannii* complex based on a mitochondrial gene tree (Verrastro et al., 2017).

Although there is no study of morphological variation across all *L. wiegmannii* populations, published data suggest a very conservative morphology that ultimately may explain why species boundaries within this complex still remain unresolved (see Etheridge, 2000, Avila, 2003, Verrastro et al., 2003, 2017, Avila et al., 2009, Cabrera et al., 2013, Villamil et al., 2017). Whether this apparently conservative morphology is reflecting limited divergence (*i.e.*, evolutionary stasis) and/or a very recent diversification is unknown. Sand dunes and open highland habitats in which *L. wiegmannii* now occurs have experienced several Cenozoic expansion-retraction cycles associated with climatic changes (Rabassa et al., 2005), which might have promoted rapid diversification in the complex driven by non-adaptive divergence in allopatry (Camargo et al., 2010). For instance, dispersal could have taken place across sand fields that expanded in the glacial periods, while vicariance may have resulted from habitat fragmentation during the inter-glacials.

Current hypotheses about *L. wiegmannii* diversification have relied on the observation of reciprocal monophyly of concatenated gene trees, an approach that ignores the expected genealogical independence among non-recombining loci. The likely recent diversification of the *L. wiegmannii* complex could have established conditions under which incomplete lineage sorting (ILS) produced discordance between gene trees and the species tree (especially if ancestral population sizes were large); reciprocal monophyly at multiple loci is unlikely to occur in such situations (Maddison, 1997; Hudson and Coyne, 2002; Zhang et al., 2011; Fujita et al., 2012). This incongruence can be explicitly modeled using the multispecies coalescent model (MSC; Rannala and Yang, 2003; Yang and Rannala, 2010, 2014). Further, new techniques for obtaining genomic data that are readily applicable to non-model organisms have revolutionized the fields of molecular systematics and phylogeography, and they are now routinely used to generate large numbers of rapidly evolving, low-cost markers for assessing questions about recent or rapid diversification (Morin et al., 2004; Helyar et al., 2011; Wagner et al., 2013; Pante et al., 2015b; Hung et al., 2016; Leaché and Oaks, 2017; Gibbs et al., 2018). For instance, ddRADseq data (Peterson et al., 2012) can be used to obtain hundreds to thousands of bi-allelic markers scattered throughout the genome, which can be directly used to infer a species tree, bypassing gene tree integration, at a relatively low computational cost (SNAPP, Bryant et al., 2012). This algorithm has been extended to delimit species using marginal likelihood estimation and model comparison using Bayes Factors (Grummer et al., 2014; Leaché et al., 2014). This approach enables statistical comparisons among non-nested hypotheses of species boundaries consisting of different numbers of species and/or different assignments of samples to species, a strategy that is not feasible with other species delimitation methods currently available (Leaché et al., 2018; Oaks et al., 2019).

In this study, we investigate the diversification of the *L. wiegmannii* complex with geographic sampling that includes most of the known populations. Our data set includes one mitochondrial gene (*cytochrome b*), three nuclear markers (KIF24, PRLR and EXPH5), and thousands of bi-allelic genomic markers obtained from ddRADseq data. We analyzed these new data using coalescent-based approaches for species tree inference and species delimitation. In addition, we also estimated divergence times in order to evaluate the hypothesis that population divergence and/or speciation events were associated with the expansion/retraction cycles of sandy habitats during the Quaternary of southern South America. Finally, we evaluated the evolutionary independence of *L. gardeli* and infer its phylogenetic position within the *L. wiegmannii* complex using *cytochrome b*, KIF24, PRLR and EXPH5 markers.

2. Materials and methods

2.1. Sampling

We obtained samples from throughout nearly the entire distribution of the *Liolaemus wiegmannii* complex (Fig. 1ii), including samples from the presumable type locality of the nominal species, near to the mouth of the Negro River at the border of the Rio Negro and Buenos Aires Provinces in Argentina (see Etheridge, 2000; black arrow in Fig. 1i). A maximum of five specimens per locality was collected by hand or a noose. Animals were euthanized by an overdose of sodium thiopental, and samples of liver or muscle and tail were taken and stored in 95% ethanol. Specimens were then fixed in 10% formalin, and deposited in the herpetological collection of the Centro Nacional Patagónico (CENPAT-CONICET), Puerto Madryn (Argentina), and the Vertebrate Zoology Collection of the Faculty of Sciences, Montevideo (Uruguay) (Table S1). All procedures followed ethical and legal requirements established in Uruguay and Argentina.

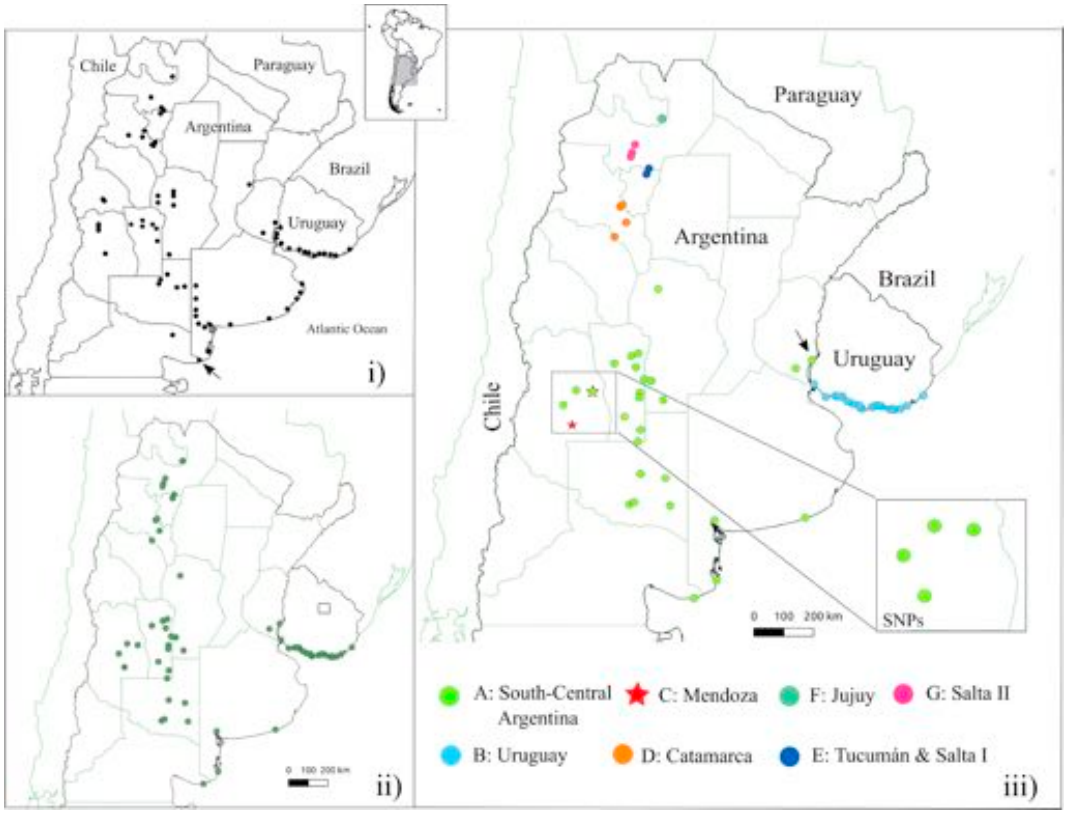

Fig. 1. (i) Distribution of the *Liolaemus wiegmannii* complex, re-drawn after Etheridge (2000), Avila et al. (2009), and Stellatelli et al. (2014). Black arrow indicates the type locality according to Etheridge (2000). (ii) Distribution of the sampled localities for this study. The square in Uruguay shows the type locality for *L. gardeli.* (iii) Distribution of the candidate species inferred for *L. wiegmannii* based on sequence and ddRADseq data. Both data sets are in general concordance with the exception of the BPP "Mendoza" clade that included the South-Central Argentina candidate species, based on genome-wide data (lower right square: "SNPs"). Light green circles: South-Central Argentina (A); Light blue circles: Uruguay (B); Red stars: Mendoza (C); Orange circles: Catamarca (D); Dark Blue circles: Tucumán & Salta I (E); Dark green circles: Jujuy (F); Purple Circles: Salta II (G). Black arrow: Las Cañas, Río Negro, Uruguay. (For interpretation of the references to colour in this figure legend, the reader is referred to the web version of this article.)

2.2. Laboratory procedures and data collection

2.2.1. Sequences

Genomic DNA was extracted mostly from liver using the NaCl-isopropanol protocol (available at: https://figshare.com/articles/MacManes_Salt_Extraction_Protocol/658946). Fragments of mitochondrial *cytochrome b* and the nuclear markers KIF24, PRLR and EXPH5 were amplified by PCR. *Cytochrome b* was amplified using IguaCytob_F2 - IguaCytob_R2 and GluDGL - Cytb3 primers developed by Corl et al., (2010), and Palumbi (1996), respectively. We used a PCR program with a touchdown of 0.3 °C per cycle for Tm: 94 °C (02:45), 35× [94 °C (00:15), 51 °C (01:00, −0.3 °C), 72 °C (01:00)], at 72 °C (07:00), following Morando et al. (2003). Each reaction "cocktail" included 18.5 µl of distilled H2O, 2.5 µl 10X buffer, 2.5 µl dNTPs (2 mM), 0.5 µl of each primer and 0.25 µl of polymerase. Nuclear KIF24, EXPH5 and PRLR fragments were amplified with the primers designed by Portik et al. (2012); KIF24_F1-R1, EXPH5_F1-R1, and Townsend et al. (2008): PRLR_F1-R3. Reactions for nuclear markers were prepared following Olave et al. (2014) and contained 8.5 µl of distilled H_2O, 1.4 µl 10X buffer, 2 µl dNTPs (2 mM), 1 µl of each primer and 0.1 µl of polymerase. KIF24 and EXPH5 were amplified through a touchdown program with three steps of cycling, where Tm decreased 0.5 °C per cycle only in the first step, following Noonan and Yoder (2009) indications: 95 °C (1:30), 10× [95 °C (0:35), 63 °C (0:35, −0.5 °C), 72 °C (01:00]; 10× [95 °C (0:35), 58 °C (0:35), 72 °C (01:00)]; 15× [95 °C (00:35), 52 °C (00:35), 72 °C (01:00)]; 72 °C (10:00). Finally, for PRLR we use a similar to CYTB program with a touchdown of 0.3 °C per cycle in Tm: 94 °C (02:45); 35× [94 °C (00:15), 51 °C (00:20, −0.3 °C), 72 °C (01:00)]; 72 °C (07:00) (Reyes-Velazco and Mulcahy, 2010).

PCR products were checked in agarose gels at 1.5X and purified using the Clean and Concentrator Kit of ZYMO (ZYMO Research Inc.) for later standard sequencing via the Macrogen service (www.macrogen.com), using the same primers employed for PCR reactions. Almost all five individuals collected per locality were sequenced for *cytochrome b*, whereas for nuclear KIF24 and PRLR markers we usually obtained sequences from three individuals, and one sequence for EXPH5.

Sequence chromatograms were visually checked and manually edited with ProSeq 3.4.7.0 (Filatov, 2009). Multiple alignments for each locus were made with Clustal X 2.0 (Larkin et al., 2007), whereas the reading frame was corroborated in MEGA 6 (Tamura et al., 2013). The specific identity of the sequences obtained was explored in GenBank via the BLAST tool. Nuclear loci were phased using the algorithm of DNASp 5.10.1 (Rozas and Rozas, 1995), and summary statistics π, S y Θ (Nei, 1987) were estimated for all loci through the same software. Finally, the fit of different substitution models for each locus was tested with jModelTest2 (Darriba et al., 2012), and the modeltest function of the phangorn package of R (Schliep, 2011).

2.2.2. Genomic data

Genomic sampling of SNPs followed the ddRADseq protocol of Peterson et al. (2012) and included 113 individuals representing all potential candidate species for the complex. DNA quality for all samples was checked in agarose gels, and DNA concentrations were measured with Qubit (Thermo Fisher Scientific). Extractions were digested with the restriction enzymes SbfI and MspI (New England Biolabs), and the obtained fragments were purified with Sera-Mag SpeedBeads beads before ligation of barcoded Illumina adaptors onto the fragments. The

oligonucleotide sequences used for barcoding and adding Illumina indexes during library preparation are provided in Peterson et al. (2012). Equal amounts of ligated DNA from each sample were combined to create a pool of individuals prior to fragment size selection using Pippin Prep (Sage Science). The final library was amplified using proofreading Taq and Illumina's indexed primers. For each pool, the fragment size distribution and concentration were assessed with an Agilent 2200 TapeStation and qPCR. Finally, libraries were sequenced in an Illumina HiSeq 2000 lane for 100 bp single-end reads via the sequencing service of the University of California (Berkeley, USA).

Primers and adapters were removed from the ddRADseq raw data using FASTX-Toolkit (Gordon and Hannon, 2010). Sequences resulted from quality filtering and de-multiplexing were then processed with STACKS 1.43 (Catchen et al., 2013), a set of programs and scripts that allows data filtering and locus identification. Reads that represented potential loci per individual were grouped using ustacks considering a minimum of coverage for grouping reads of ten (m = 10) and allowing a maximum of two mismatches (M = 2) between groups of reads. Each unique locus for all individuals was incorporated into a catalog via cstacks using a mismatch threshold of four (n = 4) and removing those loci that showed an elevated coverage, which may suggest the presence of paralogs. Haplotypes for each individual per locus were resolved with sstacks and both loci and individuals missed were filtered before final matrices were obtained via the populations tool. Different thresholds for the number of missing loci allowed were considered, as well as for the minor allele frequencies. As a final point, a single random SNP was chosen for each RAD locus, in order to avoid linkage between SNPs (Leaché et al., 2014).

A total of 1509 SNPs were obtained for 80 percent of the 113 individuals (r80), each of one having no more than 30 percent missing data (30 pMD). Reducing the SNPs present to 50 percent of individuals (r50) and the same tolerance for missing data per individual (30pMD), results in a matrix of 3912 SNPs for 75 individuals. The retention of all individuals (113) having SNPs at least for 50 percent of them is only possible under higher tolerance of missing data per individual. For instance, r50 with a pMD of 50 (50 pMD) retain 3912 SNPs for 113 specimens. This trade-off between the number of SNPs retained and the sample size (number of individuals), is expected for RADseq data (Leaché et al., 2014 and references therein).

2.3. Sequence-based species delimitation and divergence times estimates

In order to assign individuals to candidate species, Bayesian and Maximum Likelihood *cytochrome b* genealogies were inferred with Beast 1.8.4 (Drummond et al., 2012) and RAxML *v.* 8 (Stamatakis, 2014) respectively, using *Liolaemus lutzae* as an outgroup. Beast was run with a Yule model as a prior of the tree, assuming an uncorrelated lognormal relaxed clock with a HKI + G substitution model. RAxML analysis was conducted with a GTRGAMMA model, and node support was assessed through 1000 bootstrap replicates. From these genealogies, single locus species delimitation was carried out with GMYC (Pons et al., 2006) and mPTP (Kapli et al., 2017). All individuals of a given cluster supported by mPTP and GMYC with also posterior probabilities > 0.95 or bootstrap support > 75 in the gene trees, were assigned a priori to the same candidate species. These candidate species were subsequently tested in BPP 3.4 (Yang and Rannala, 2014) based on the four loci. BPP analyses were run under the A11 configuration (joint species delimitation and species tree inference), which is an unguided species delimitation (Yang, 2015). Ploidy variation among loci was taken into account through heredity scalar settings of 1 for KIF24, PRLR and EXPH5, and 0.25 for *cytochrome b*. Locus substitution rates were estimated with a Dirichlet distribution $D(\alpha)$, with $\alpha = 2$, which reflect rate differences among loci. Finally, a flag indicating unphased nuclear loci was included in the control file via the diploid option.

Taking into account that BPP can result sensitive to Θ and τo prior distributions (Zhang et al., 2011), these were parametrized through Inverse Gamma distributions (Inv-Gamma(α, β)) considering $\alpha = 3$ and values of β that cover different alternative scenarios for ancestral population size and root age (Ruane et al., 2014, Grummer et al., 2014): (a) Θ = Inv-Gamma(3, 0.2) and τo = Inv-Gamma(3, 0.2): large population size and deep divergence; (b) Θ = Inv-Gamma(3, 0.002) and τo = Inv-Gamma(3, 0.002): small population size and shallow divergence; (c) Θ = Inv-Gamma(3, 0.2) and τo = Inv-Gamma(3, 0.002): large population size and shallow divergence; and (d) Θ = Inv-Gamma (3, 0.002) and τo = Inv-Gamma(3, 0.2): small population size and deep divergence, where (c) is the most conservative speciation scenario (Leaché and Fujita, 2010). Each pair of Θ and τo prior settings were run under four alternative starting tree topologies, and each combination of these factors was run four times using different random seeds in order to check convergence among runs.

Divergence times for the lineages supported by BPP were estimated in *BEAST (Drummond and Rambaut, 2007), which infer divergence times under the multispecies coalescent, emphasizing incomplete lineage sorting as the principal source of gene-species tree discordance (Heled and Drummond, 2010). This analysis was run assuming uncorrelated lognormal relaxed clocks, and used the substitution rates estimated by Olave et al. (2015) for *Eulaemus* (*cytochrome b*: 1.9355×10^{-2} ($\pm 3.4639 \times 10^{-5}$); PRLR: 1.3223×10^{-3} ($\pm 2.9225 \times 10^{-6}$); KIF24: 1.9021×10^{-3} ($\pm 3.5705 \times 10^{-6}$); EXPH5: 1.2955×10^{-3} ($\pm 0.2806 \times 10^{-6}$)). Gamma and Inverse Gamma distributions were used for the priors of species.Pop.mean and species.yule.Birth.rate. Under Gamma prior, shape (α) and scale parameter ($1/\beta$) where, respectively, setting in 2 and 1/2000 for species.pop.Mean, and 1 and 1/10 for species.yule.Birth.rate. Inverse Gamma distribution was only used for species.pop.Mean, with an initial value of 0.015, and shape and scale of 3 and 0.3, following Grummer et al. (2014). When Inverse Gamma was used for species.pop.Mean, species.yule.Birth.rate was set as the default.

For both BEAST and *BEAST analyses, stationarity of Markov chain and effective sampled sized (ESS) for each estimated parameter were assessed with Tracer v1.6 (Rambaut and Drummond, 2007), where parameter estimates were considered robust enough when traces reached stationarity, and ESS values were greater than 200. All generations before stability were discarded.

Runs generated 10,000 trees that were summarized with TreeAnnotator (Drummond and Rambaut, 2007), discarding the first 1000 trees. The annotated tree that resulted from this step was finally visualized in FigTree v1.4.2 (available at: http://tree.bio.ed.ac.uk/software/figtree/).

2.4. Genome-wide species limits, genomic variation and species tree estimation

The SNP matrix that includes 3912 loci for 113 individuals was transformed to a *genind* class object in the adegenet package (Jombart, 2008) of R 3.5.0 (R Core Team 2018), with which it is possible to analyze thousands of SNPs at low computational costs. From this object we ran a Principal Component Analysis to explore the general structure of the dataset. SNP clusters ranging from K = 1 to 20 were evaluated through the *snapclust.choose.k* function of adegenet using AIC and BIC. Best K values were then considered for a Discriminant Analysis of Principal Components (DAPC). Finally, membership probabilities of each individual to the DAPC clusters were inspected through the *compoplot* function of adegenet.

In addition, a maximum likelihood SNP-based tree was inferred with RAxML-NG (Kozlov et al., 2018) using a GTR + G + ASC_LEWIS model, 100 starting trees and 1000 bootstrap replicates to assess node support. Given that SNPs only contain variable sites, the ASC option was used to correct for an ascertainment bias in the likelihood calculations.

Both adegenet and RAxML-NG analyses were used to assign individuals to putative species for subsequent testing with a Bayes Factor

Species Delimitation approach (Leaché et al., 2014). This allows comparing alternative species delimitation hypotheses under the Multispecies Coalescent Model based on marginal likelihood estimations. Bayes Factor Species Delimitation (BFD*) was implemented via the SNAPP (Bryant et al., 2012) and Path Sampler packages of BEAST 2.5 (Bouckaert et al., 2014). A matrix composed by 3912 SNPs and 113 individuals was transformed to the SNAPP format with Phrynomics (https://github.com/bbanbury/phrynomics), allowing the inclusion of original missing data. Missing loci per individual were counted through a while loop with egrep in Bash. Then, considering six individuals for each of the candidate species suggested by the adegenet and RAxML analyses, those individuals with the fewest missing loci were retained in a new matrix. Each locus was inspected for missing data with a spreadsheet, in which a value of 1 was assigned to those loci present in all individuals; otherwise, a missing locus was flagged with a value of 0. This information was used to process the 3912 loci × 36 individuals matrix with a for loop in R 3.5.0, which transferred only those loci labeled with 1 to a new file. At the end of the pipeline, we obtained a matrix of 214 loci for 36 individuals with no missing data.

SNAPP mutation rate parameters u and v were set to 1, and the coalescent rate was sampled from the prior with an initial value of 10. Speciation rate of the Yule model (λ) and Θ were parametrized through Gamma prior distributions with $\alpha = 2$ and $\beta = 200$ for λ, and $\alpha = 1$ and $\beta = 250$ for Θ. Marginal likelihood for each model was estimated through Path Sampling considering 40 steps, with an MCMC length of 400,000 for each step, a pre-burning of 40000, and 10% of final burning. This MCMC sampling frequency was sufficient to ensure that the majority of ESS values were > 200. Marginal likelihood values were then used to compare alternative models of species limits via Bayes Factors ($2log_e$BF), calculated as twice the difference in marginal likelihood between two models: $2log_e\text{BF} = 2(MLE(model_1)\text{-}MLE(model_2))$. The strength of support for a model was assessed following the framework of Kass and Raftery (1995) in which $2log_e$BF values between 6 and 10 strongly support model 1 over 2, and values above 10 decisively support model 1 over 2. Finally, the species tree of the best-ranked model was summarized with TreeAnnotator, discarding the first 1000 trees.

Both Marginal Likelihood estimates for BFD* and Maximum Likelihood tree inference with RAxML-NG were conducted in a linux supercomputer cluster composed of 28 nodes with 20 CPUs (40 cores), and ~125 Gb of RAM each (National Supercomputing Center ClusterUY, www.cluster.uy). For BFD*, RAM and CPU usage varied across models, but in general, the more species the model has, the more RAM and computing time it requires. For instance, 6 species models required 7 days, allowing the use of 20 CPUs (2 core each) and 125 Gb of RAM. The RAxML SNPs tree inference took ~ 18 h with 10 CPUs and 10 Gb of RAM through 5 threads.

The topology of the SNP-based species tree was also inferred with SVDquartets (Chifman and Kubakto, 2014), for which 1509 and 3912 SNPs matrices were used. SVDquartets is a recently developed method of species tree estimation under the multispecies coalescent that uses site patterns to estimate unrooted topologies based on quartet taxa relationships. SVDquartets assess the uncertainty in species relationships via non-parametric bootstrapping, and has been recently incorporated to PAUP 4.0 (Swofford, 1998). Using a standard computer, this software can estimate a species tree topology for thousands of SNPs and 100 individuals in minutes, which makes it an excellent tool for recovering species trees once the limits between lineages have been previously inferred.

3. Results

3.1. Summary statistics and substitution models

We obtained 162 sequences of *cytochrome b*. Fragment lengths differed between primers; PCR amplicons obtained with IguaCytob F-R are almost 300 bp longer than those amplified with GluDGL-Cytb3. Final alignments for *cytochrome b* were 743 bp in length. Nuclear loci were sequenced for a subset of individuals with the following results: 98 sequences were obtained for KIF24, 47 for PRLR, and 19 for EXPH5. Final alignments for these markers were 420 bp, 370 bp and 737 bp length, respectively. *Cytochrome b* exhibited the highest variability of the four loci sequenced, on average having an order of magnitude greater variation than KIF24, EXPH5 and PRLR. According to Bayesian Information Criteria (BIC), the HKI model was the best fit for all loci (Table 1).

Table 1
Summary data for the four loci amplified for the *Liolaemus wiegmannii* complex. S: number of polymorphic sites; π: nucleotide diversity (expressed as the average number of pair differences); Θ_w: Watterson's Theta.

Locus	Length	Model	S	π	Θ_w
CYTB	743 bp	HKY + G	156	0.03997	0.03709
KIF24	420 bp	HKY	50	0.01208	0.02052
PRLR	370 bp	HKY	19	0.00342	0.01004
EXPH5	737 bp	HKY + I	25	0.00491	0.00807

3.2. Cytochrome b genealogy and single locus species delimitation

No topological differences are observed between the ML and Bayesian CYTB gene trees; both BEAST and RAxML (not shown in Fig. 2) analyses recovered seven strongly supported haploclades. Three haploclades are novel for the *L. wiegmannii* complex, corresponding to populations from Tucumán, Salta, and Jujuy Provinces (Argentina); these localities were not included in earlier molecular studies of this species complex. Further, two well-supported haploclades were found in Uruguay; one occurs in the locality of Las Cañas (Department of Río Negro) to the north of the Negro River (black circles in Fig. 2, black arrow in Fig. 1iii), and is widely distributed throughout south-central Argentina. The second haploclade of Uruguay is exclusively distributed along the shores of the lower Uruguay River, the La Plata River, and along the Atlantic Coast from south of Negro River to west of the Valizas creek (light blue in Fig. 2). Structure is also resolved within the south-central Argentinean lineage (light green in Fig. 2) because many haplotypes are recovered in well-supported groups, but none of them has geographic correspondence.

Single locus species delimitation with mPTP supports five of the seven haploclades resolved in the gene tree, combining (C + D) and (F + G) as single candidate species (Fig. 2). However, the GMYC, supports (C + D) and (F + G) as separate species, and also recovers other unsupported candidate species nested within A and B (light gray blocks in Fig. 2).

We collected CYTB data for only four individuals of the recently described *L. gardeli* (not included in Fig. 2), and these four sequences have only one polymorphic site. When these are included in the genealogy, *L. gardeli*, south-central Argentina (A) and Uruguay (B) are recovered as a strongly-supported haploclade (PP = 0.98), although the relationships among these three lineages are not resolved [PP (Uruguay, South-Central Argentina) = 0.63] (Fig. S1). Finally, there are two unique CYTB haplotypes (not shown in Fig. 2), that when considered are recovered closer to *L. gardeli* than the South-Central Argentina haplotypes, although without support (Fig. S1). One of these (LJAMM 13266), occurs 25 km north of Villa Mercedes in the Department of General Pedernera (San Luis Province), and might be an ancestral polymorphism of the South-Central lineage. The other haplotype (LJAMM 3132), represents the only individual that we collected in the locality of Copacabana in the Sierras de Córdoba (Province of Córdoba), part of the Chaco Serrano region where the species was historically known to occur from several localities at about 900 m, but individuals are now hard to find (LJA personal observation). These two haplotypes

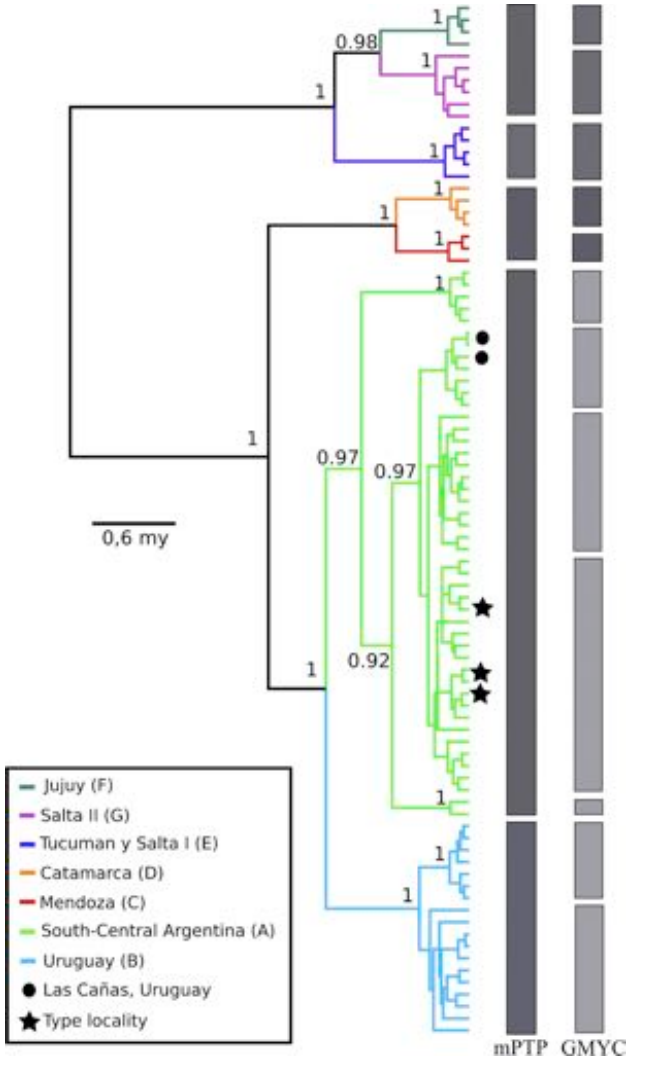

Fig. 2. Bayesian *cytochrome b* genealogy of the *Liolaemus wiegmannii* complex and results of species delimitation with mPTP (left column) and GMYC (right column). Darker grey blocks identify distinct candidate species, strongly supported by these methods, whereas lighter blocks identify unsupported splits. Seven main haploclades are identified by different colors, and their general distributions are indicated in the lower left box. Black circles identify haplotypes present in Las Cañas, Uruguay, and black stars identify haplotypes from the type locality area of *L. wiegmannii* suggested by Etheridge (2000). Numbers above branches represent posterior probabilities and the scale bar correspond to 0.6 million years. The tree was rooted with *L. lutzae* as outgroup.

were included as part of the South-Central Argentina candidate species in the subsequent delimitation and species tree analyses.

3.3. Species limits

3.3.1. Sequence-based species limits

An eight species model is inferred by BPP under three of the four scenarios (**a–d**) with varying priors for Θ and *τo*. However, posterior probabilities for eight species were > 0.95 for **b** and **d** only. The most conservative scenario (**c**), suggests eight species with an associated posterior probability < 0.95, which is likely related to the uncertainty of candidate species F and G. Finally, seven species are suggested under scenario **a**, which implies F and G are conspecific, although there is no support for neither the model nor the (F + G) candidate species (Table 2). Candidate species A, B, E and *Liolaemus gardeli* are strongly supported under all the scenarios explored, although it is important to note that we included only four individuals of *L. gardeli*. Furthermore,

Table 2
Posterior probabilities for the candidate species (A-G and *L.* gardeli) delimitated by BPP 3.4 under four scenarios for Θ and τ. Runs were conducted using four different starting trees and replicated under four alternative seeds. a) Θ = Inv-Gamma(3, 0.2) and *τo* = Inv-Gamma(3, 0.2); b) Θ = Inv-Gamma(3, 0.002) and *τo* = Inv-Gamma(3, 0.002); c) Θ = Inv-Gamma(3, 0.2) and *τo* = Inv-Gamma(3, 0.002); d) Θ = Inv-Gamma(3, 0.002) and *τo* = Inv-Gamma(3, 0.2). *N Sps* is the number of species delimited and *PP N* the associated posterior probability of the model. A: South-Central Argentina; B: Uruguay; C: Mendoza; D: Catamarca; E: Tucumán-Salta I; F: Jujuy; G: Salta II. Values reported here correspond to one replicate. All results across the different starting trees and seed used are shown in Table S2.

Θ and τ	*N Sps*	*PP N*	A	B	C	D	E	F	G	*L. gardeli*	FG
a	7	0.62	1	1	0.86	0.86	1	0.34	0.34	1	0.66
b	8	1	1	1	1	1	1	1	1	1	0
c	8	0.63	1	1	0.95	0.96	1	0.66	0.66	1	0.34
d	8	1	1	1	1	1	1	1	1	1	0

candidate species C and D are supported in three of the four scenarios explored, and F and G have strong support in two of these (Table 2). Despite high convergence among runs, both **b** and **d** priors returned a seven species model under the topology 3 of the starting tree [(((A, B), H), ((C, D), (E, (F, G))))] with a posterior probability of ~0.6 and 0.9, respectively. Again, this seven species model resolves (F + G) as one species (Table S2).

Seven of the eight candidate species resolved in the most frequently supported model occur in allopatry (Fig. 1iii). Spatial overlap between the widely distributed lineage of the South-Central Argentina (light green) and the Mendoza lineage (red star) occurs at a single locality in La Paz, Mendoza, Argentina (km 276 of the national route 146) both candidate species can be collected in the same sand dune area.

3.3.2. Genome-wide species limits and genomic variation

Principal Component Analysis based on 3912 SNPs suggests six main groups of individuals that largely correspond to the A + C, B, D, E, F and G candidate species supported by BPP (Fig. 3i). Individuals from South-Central Argentina (A + C) and Uruguay (B) are clearly separated from northern individuals of Catamarca (D), Tucuman & Salta I (E), Jujuy (F) and Salta (G) along the first principal component. Differentiation within these two groups is also observed along the second principal component ([AC + B] and [D, E, F, G]; Fig. 3i). The *snapclust.k* function of adegenet suggests between 5 and 6 clusters considering BIC and AIC respectively (Fig. S2), which in general is consistent with the structure observed in the PCA, and corresponds to A (+C), B, D, E, F and G lineages from BPP. From this structure of six clusters, DAPC shows a clear differentiation of most of the groups. Lineage assignments A-G were included as a proxy, and all the individuals belonging to the C lineage identified in BPP, are totally overlapped with individuals from A (Fig. 3ii, Table S3). No admixture is observed between clusters (Fig. 3iii). Again, all the individuals from the Mendoza (C) lineage of BPP, show a membership probability of 1 to the South-Central Argentina (A) cluster. This last group and Uruguay (B) appear very close in both PCA and DAPC (particularly), which might suggest that under K = 5, A and B would belong to the same group (Fig. 3i and ii). However, no admixture between A and B is recovered by adegenet (Fig. 3iii), and consequently, we kept K = 6 for subsequent analyses.

A maximum likelihood tree based on 3912 SNPs strongly supports lineages B, D, F and G as monophyletic (Fig. 4i). A + B is also supported, however, there is no reciprocal monophyly between A and B lineages; A is paraphyletic with respect to a monophyletic B, and again it includes all the individuals of C (with genomic data). The monophyly of (E + (F, G)) is also recovered, but the reciprocal monophyly of E respect to the (F, G) clade is not well supported.

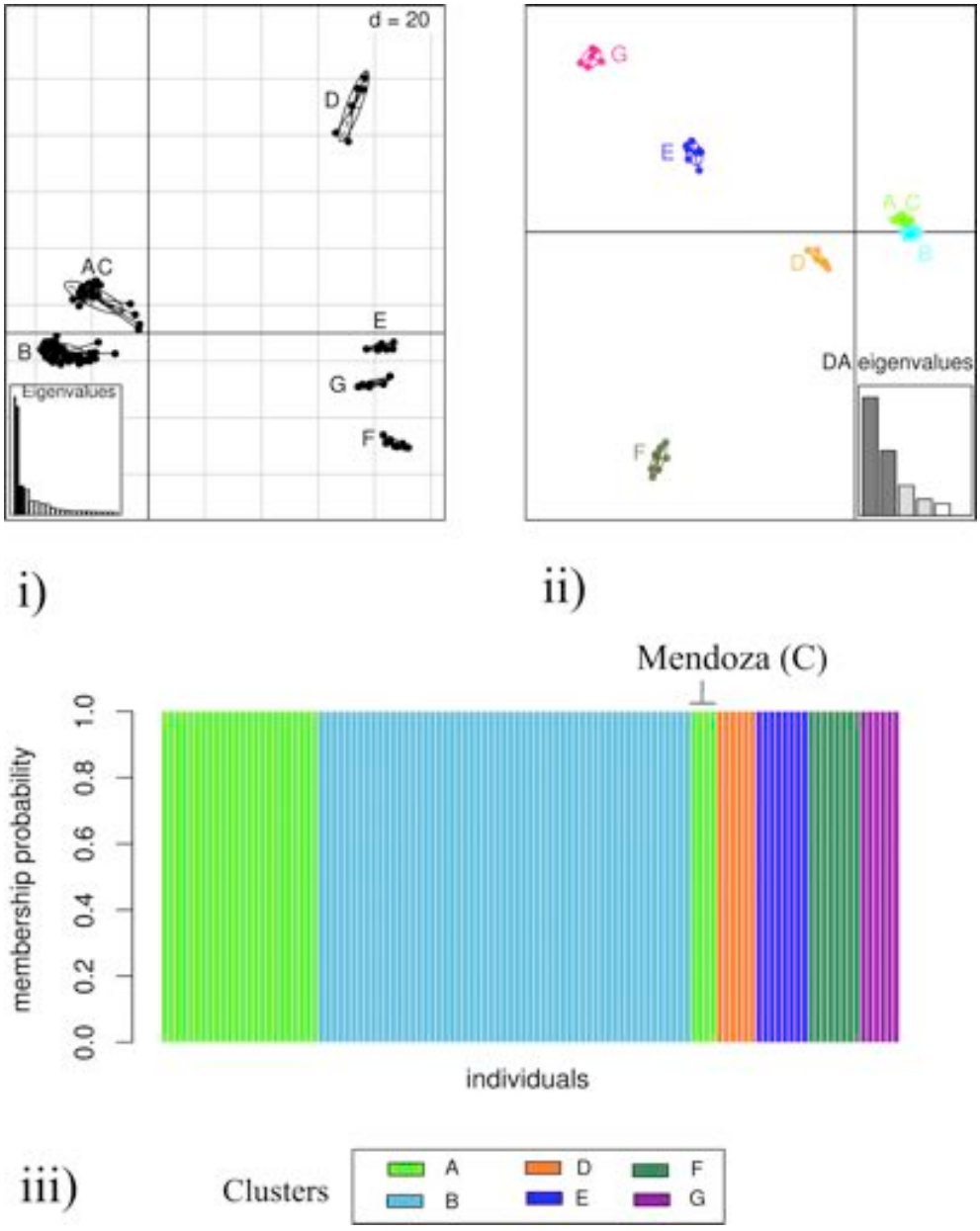

Fig. 3. Results of PCA and DAPC analyses of *Liolaemus wiegmannii* complex from 3912 SNPs. Bi-dimensional projection of the genomic variation summarized by the Principal Component analysis (i) and the Discriminant Analysis of Principal Components (ii). Membership probabilities of each individual to the clusters of DAPC (iii). A: South-Central Argentina; B: Uruguay; D: Catamarca; E: Tucumán-Salta I; F: Jujuy; G: Salta II.

Bayes Factor Species Delimitation decisively supports Model 1 –six candidate species for the *Liolaemus wiegmannii* complex– over all other alternative hypotheses. Model 4, in which candidate species A and B are conspecific, is the second best-ranked model, which is consistent with DAPC and ML tree result that suggest the possibility of 5 groups within the complex. Even so, model 1 is decisively supported over the above model by a $2log_eBF$ of +305.45 (Table 3).

3.4. Species tree topology

3.4.1. Sequence-based species tree estimation

Taking into account the maximum splitting scenario supported by BPP, only the (A, B) and (E, (F, G)) clades are strongly supported in the species tree inferred with *BEAST; these results are independent of the prior parametrization of species.PopMean and the species.yule.birthrate used. The (C, D) relationship is also recovered under the priors mentioned above, although it is not well supported. Under Gamma priors for species.PopMean and species.yule.birthrate, the (C, D) clade is recovered as sister to (A, B), whereas for Inverse Gamma (C, D) is placed sister to (E, (F, G)), although both relationships are weakly supported (Fig. 5i and ii).

Moreover, lumping lineage C (Mendoza) with A (South-Central Argentina) as suggested by the SNP data, does not impact the support of (E, (F, G)) and (A, B) clades for both Gamma and Inverse Gamma priors (Fig. 5iii and iv). For this seven species scenario, lineage D (Catamarca) is recovered as sister of (*L. gardeli* (A, B)), although the support for this relationship is low.

Liolaemus gardeli is clearly nested within the *Liolaemus wiegmannii* complex, but its position has only moderate support under Inverse Gamma prior for species.PopMean (Fig. 5ii).

3.4.2. Genome-based species tree estimation

Species tree estimation of Model 1 from BFD* recovered a strongly supported dichotomy between (A, B) and (D, (E, (F, G)) clades, which

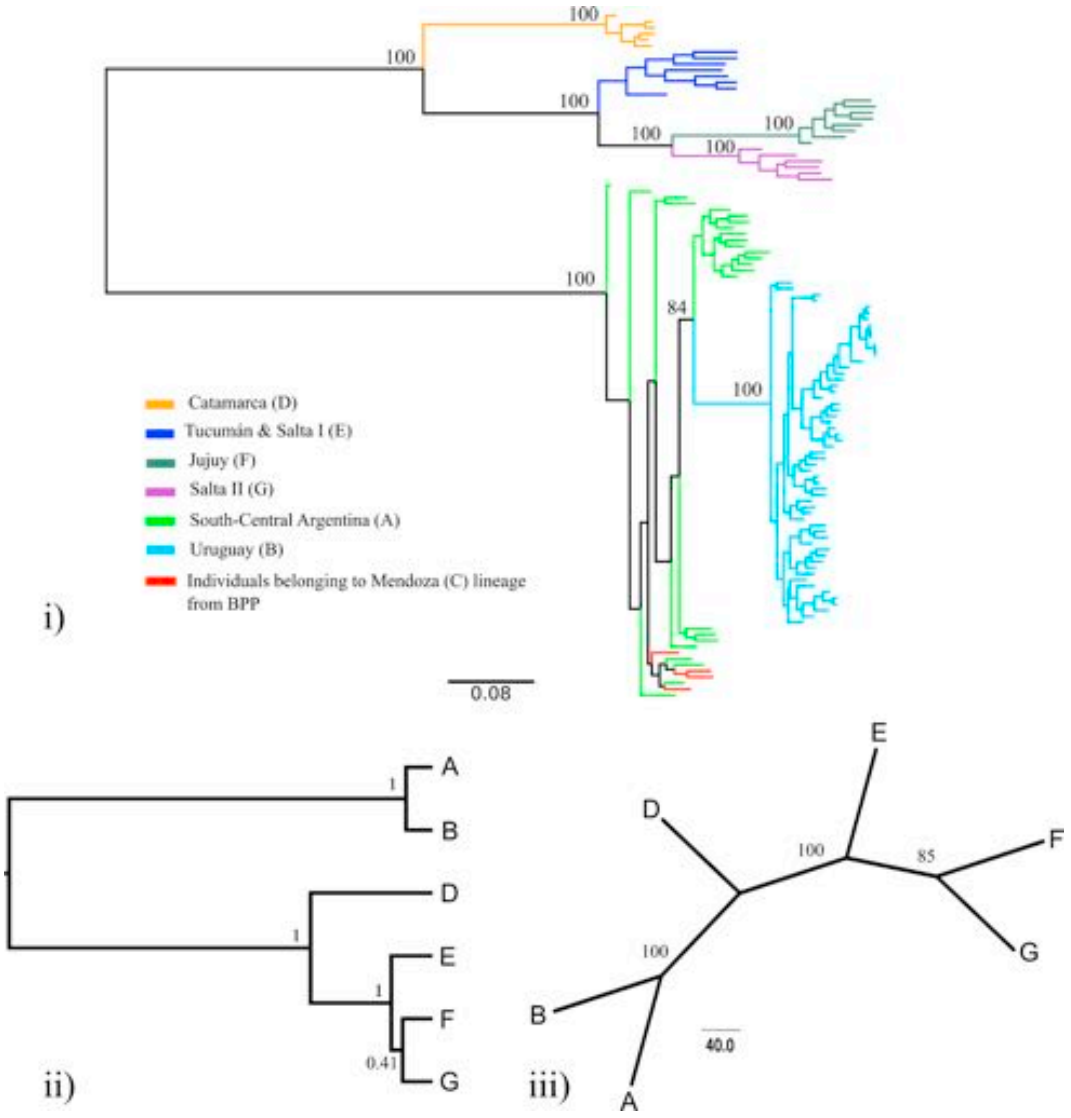

Fig. 4. Maximum likelihood and species trees of the *Liolaemus wiegmannii* complex based on ddRADseq data. (i) Maximum Likelihood tree inferred from 3912 SNPs with RAxML-ng. Numbers above nodes represent bootstrap support (values below 75 are not shown). Lineages A-D are represented in the same colors as in Fig. 2, and their general distribution is presented in the interior left box. Individuals from C (red branches) are nested within A. (ii) SNAPP species tree inferred with 214 SNPs and the Model 1 from BFD*, which considered the six distinct candidate species. Numbers above branches are posterior probabilities. (iii) SVDquartet species tree of the 6 species delimited from BFD*, estimated with 3912 SNPs. Numbers above branches represent non-parametric bootstrap values. A: South-Central Argentina; B: Uruguay; C: Mendoza; D: Catamarca; E: Tucumán-Salta I; F: Jujuy; G: Salta II. (For interpretation of the references to colour in this figure legend, the reader is referred to the web version of this article.)

Table 3
Bayes Factor Species Delimitation results for the *Liolaemus wiegmannii* complex using a matrix composed of 214 SNPs with no missing data and 36 individuals. Model 1 represents the most species-rich scenario suggested by PCA, DAPC and Maximum likelihood inference (6 candidate species: A: South-Central Argentina; B: Uruguay; D: Catamarca; E: Tucumán-Salta I; F: Jujuy; G: Salta II). Subsequent models derive from lumping two or more of these lineages.

Model	Species	Marginal Likelihood	Rank	$2log_eBF$
1	6: A, B, D, E, F, G	−3299.7	1	–
2	5: A, B, D, E, FG	−3519.4	4	+439.46
3	5: A, B, D, EG, F	−3492.2	3	+385.02
4	5: AB, D, E, F, G	−3452.4	2	+305.45
5	4: AB, D, E, FG	−3672.4	6	+745.48
6	4: AB, D, EG, F	−3644.8	5	+690.23
7	3: AB, D, EFG	−3870.1	8	+1140.7
8	4: A, B, D, EFG	−3717.9	7	+836.34
9	2: AB, DEFG	−4911.1	9	+3222.8
10	2: ABD, EFG	−5969.5	10	+5339.6

resolves the basal polytomy observed in the sequence-based species tree. Monophyly of northernmost lineages (E, (F, G)) is also recovered, relationships among these three are unresolved (Fig. 4ii). Finally, the unrooted species tree estimated by SVDquartet is in general concordance with both the SNAPP tree and the sequence-based *BEAST topology, (A, B) and (E, (F, G)) nodes strongly supported by bootstrap values of 100. The relation (F, G) is also well supported although with lower bootstrap value than the mentioned above (Fig. 4iii).

3.5. Divergence times

Divergence time estimates by *BEAST suggest that early diversification of the complex occurred during the Lower Pleistocene, between 1.27 (HPD 95%: [0.82-1.80]) and 1.41 (HPD 95% [0.98-1.98]) million years before present (YBP). Within strongly supported lineages, divergence took place in the Middle Pleistocene. The candidate species from Uruguay (B) diverged from its sister species in south-central Argentina (A) between 310 (HPD 95%:[131-575]) and 342 (HPD 95%:[147-573])

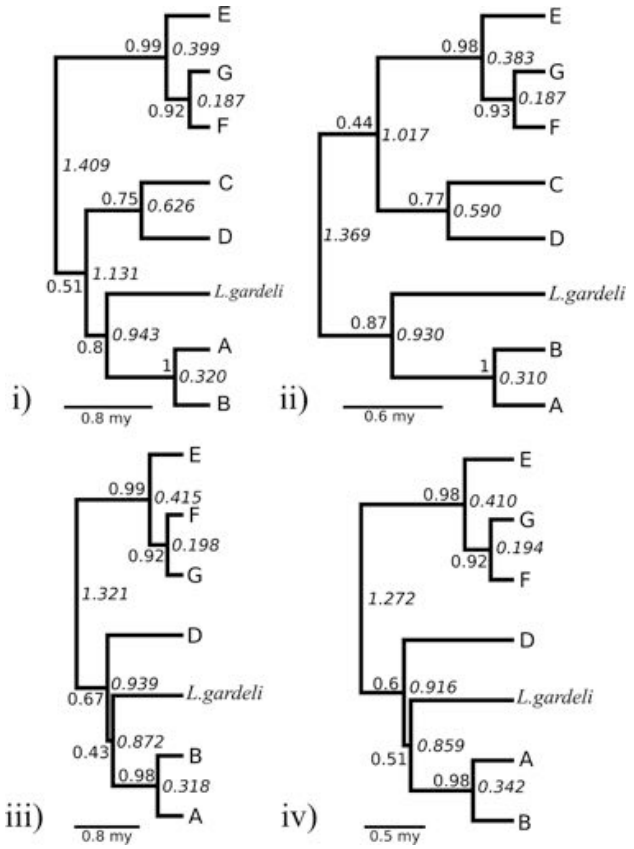

Fig. 5. Species tree and divergence times for the *Liolaemus wiegmannii* complex inferred from *cytochrome b*, KIF24, PRLR and EXPH5. (i) and (ii) considered the eight species delimited by BPP, whereas (iii) and (iv) lumped C with A. Priors for species.pop.Mean and species.Yule.birth.rate were parametrized with Gamma (i and iii) and Inverse Gamma (ii and iv). Posterior probabilities are shown above or below branches whereas divergence times are shown next to the nodes, in italics. A: South-Central Argentina; B: Uruguay; C: Mendoza; D: Catamarca; E: Tucumán-Salta I; F: Jujuy; G: Salta II.

thousand YBP, whereas divergence between Tucumán and Salta I (E) and the pair Jujuy and Salta II (F, G) range from 383 (HPD 95%: [196-634]) and 415 (HPD 95%: [211-679]) thousand YBP. Finally, the split of Jujuy (F) from Salta II (G) had been taking place between 187 (HPD 95%: [70-363]) and 198 (HPD 95%: [73-389]) thousand YBP (Fig. 5).

4. Discussion

4.1. Species limits

We find strong evidence of a species complex for *L. wiegmannii,* which is in general agreement with the results of Avila et al. (2009). Three of the four lineages resolved by Avila et al. (2009) are recovered as distinct candidate species with our multispecies coalescent approach based on both sequence and ddRADseq data: *L. wiegmannii, L. wiegmannii* Uruguay, and *L. wiegmannii* Catamarca [here identified as: A (South-Central Argentina), B (Uruguay), D (Catamarca) respectively]. The *L. wiegmannii* Mendoza from Avila et al. (2009) [here called: C (Mendoza)] is supported only by the BPP analysis based on sequence data. Both the ML SNP-based tree and DAPC clearly show that "Mendoza" individuals belong to the "South-Central Argentina" lineage, which suggests that this pattern is probably the result of deep coalescence of *cytochrome b* haplotypes. Other potential ancestral polymorphisms in the *cytochrome b* are also observed in this lineage, but at lower levels of divergence (LJAMM 13266 and 3132, see Fig. S1 and Table S3). The three northernmost *L. wiegmannii* lineages (E, F and G) are supported as distinct species by BPP and *BFD, although under two scenarios for Θ and τ in BPP, posterior probabilities of F and G are well below 0.95, which suggest that F and G be conspecific. Even so, BFD* decisively supports a model of six candidate species, (which are suggested by DAPC and the RAxML tree), over the model that lumps F and G together. Populations of the E, F, G lineages were previously known (Etheridge, 2000), but remained unexplored from a molecular perspective until this study. In addition, the second best-ranked BFD* model implies that A and B represent a single candidate species, which is concordant with the paraphyly of A recovered in the RAxML tree, the proximity of A and B in the PCA and DAPC plots, and the K = 5 value inferred with BIC. Although BFD* could overestimate species limits, no admixture between individuals of A and B was observed. Collectively these results suggest incipient speciation for A and B, possibly involving large ancestral population sizes.

Sukumaran and Knowles (2017) point out that genome-wide data could inflate species-level diversity given its power to detect fine-grained population genetic structure. In this study however, the detailed genomic data, enabled us to limit overestimation of candidate species (*i.e.,* considering "Mendoza" as a distinct lineage) that would result from the use of coding sequences alone. Nevertheless, our study is not exempt from the limitations of the Multispecies Coalescent approach when infraspecific genetic structure is strong (see Sukumaran and Knowles, 2017), and therefore the candidate species presented here should be taken as working hypotheses. Despite these limitations, the multispecies coalescent is the most objective approach available to explore species limits using multi-locus sequence and genome-wide data (Fujita et al., 2011; Fujita et al., 2012; Leaché et al., 2014, 2019). Additional empirical evidence for delimiting species may still be needed in our study, given that all candidate species supported by *BFD occur in allopatry (Leaché et al., 2019). In this sense, the contrasting environments in which the northernmost lineages (E, F and G) occur with respect to A and B (*i.e.,* sub-Andean sedimentary formations surrounded by a transitional dry Chaco vegetation, *vs.* extensive northern Patagonian, Pampean and coastal sand dune regions) might suggest some grade of ecological differentiation among them, but further study is needed.

Empirical studies often show that BFD* tends to favor the "most species-rich" models (Battey and Klicka, 2017; Nieto-Montes de Oca et al., 2017; O'Connell et al., 2018; O'Connell and Smith, 2018; Noguerales et al., 2018), although there is no strong relationship between the species richness in delimitation models and their MLE values (Leaché et al., 2018). Independently from the potential oversplitting trend of the method, this bias in BFD* seems to be caused by differences in the number of loci retained for each competing model when missing data are included (Leaché et al., 2018). Given that SNAPP will remove loci not shared among all the species in the model, those with more species will have fewer loci and will rank better in marginal likelihood estimates (Leaché et al., 2018; Noguerales et al., 2018). Consequently, models with different numbers of loci are not comparable because their differences in MLE are not related to the probability of each competing model given the same data. We explored this problem here using an alternative dataset of 595 SNPs that allows 5% missing data. As expected, as different numbers of loci were removed by SNAPP in each model, a strong correlation between the number of SNPs and the marginal likelihood estimates was observed (Appendix A). In fact, this matrix led to the decisive retention of an arbitrary split model over the model supported by our discovery methods (*e.g.,* DAPC or RAxML). For instance, a model that arbitrarily split B into two species was decisively favored over the model that assumed B as a single species, by a $2log_eBF$ value of +311.4. However, when this "arbitrary split" scenario is analyzed using the matrix without missing data, BFD* strongly supports the six species model over the arbitrary split model with a $2log_eBF$ = +10.03. Although this $2log_eBF$ is not fully in the range of a decisive choice, clearly illustrates how the inclusion of missing data could lead to the retention of different numbers of loci, and artificially inflate MLE differences between models (compare Table 3 and Appendix A).

4.2. Phylogeny and diversification of the complex

4.2.1. Phylogeny

The species tree based on sequence data recovers the three northernmost candidate species of the complex (E, F and G) as monophyletic with high support. Within this clade, Tucumán and Sierra de la Candelaria (E) lineage is recovered as the sister clade of the [Cachipunco and Sierras de Santa Bárbara (F) + localities at the Department of Guachipas and Coronel Moldes in Salta (G)] clade. The [South-Central Argentina (A) + Uruguay (B)] clade is also strongly supported, but this clade forms a basal polytomy with Catamarca (D) and *Liolaemus gardeli*. In this case short internal branches and lack of support could result from either: (1) rapid diversification due to roughly simultaneous lineage splitting (*i.e.*, "hard polytomy"), which cannot be resolve with additional data; or (2) a "soft polytomy" (Hoelzer and Melnick, 1994; Rokas et al., 2005), which may be resolved with additional data. Several recent studies have used RADseq data to resolve phylogenetic uncertainties in taxa that have diversified at both deep and shallow timescales (Wagner et al., 2013; Díaz-Arce et al., 2016; Herrera and Shank, 2016; Wang et al., 2017). However, the utility of RADseq data to resolve polytomies at "deep" phylogenetic scales may be limited by "locus dropout" and a high proportion of missing data (Lee et al., 2018).

Despite these limitations, we show that ddRADseq data has the power to resolve topological uncertainties in the recent diversification of the *Liolaemus wiegmannii* complex; the basal polytomy between (E, (F, G)), (A, B) and D is recovered by SNAPP in a fully resolved nested hierarchy as: (D, (E, (F, G))) and (A, B). Although uncertainty remains within the clade (E, (F, G)) in the SNAPP tree, (F, G) is strongly supported in the SVD quartet tree, which is based on about ten times more SNPs than the SNAPP tree. Future inclusion of RADseq data for *L. gardeli* will be essential for a better understanding of the *L. wiegmannii* complex species tree.

4.2.2. The diversification of the complex

Divergence time estimates show that the *L. wiegmannii* complex diversified during the Pleistocene, suggesting that the conservative morphology observed might derive from this very recent diversification. However, we cannot rule out selective pressures favoring the apparent morphological conservatism in the complex. The final resolution of the species tree and the application of phylogenetic comparative approaches will be necessary in future studies to infer the evolutionary processes that may have constrained morphological divergence in the complex.

Pleistocene diversification has been hypothesized for several Patagonian *Liolaemus* species complexes (Morando et al., 2004, 2007; Breitman et al., 2011a, 2012; Medina et al., 2015, 2017), possible driven by the climatic changes that characterized this period (Morando et al., 2004, Breitman et al., 2012, Fontanella et al., 2012). Climatic changes (*i.e.,* glaciations) have almost certainly played a major role, especially at higher latitudes (*e.g.*, Patagonia), but habitat changes at intermediate latitudes of South America have also been recorded (Tonni et al., 1999, Rabassa et al., 2005), albeit these are also likely secondary effects of recurrent glaciations. In particular, expansion of sand dune fields over northern Patagonia and Pampas has been documented for the Last Glacial Maximum (Iriondo, 1999), and probably represented a recurrent pattern across other Cenozoic glaciations (Rabassa et al., 2005). For instance, a number of fossil assemblages suggest the aridization of the Pampas associated with the Great Patagonian Glaciation (Soibelzon and Tonni, 2009). The first divergence event in the complex largely coincides with the Great Patagonian Glaciation (~1.68–1.02 my) (Rabassa et al., 2005), and our genome-wide species tree suggests that this event split the complex in two main groups: one including all lineages associated with sub-Andean sedimentary formations, and the other including the "sand fields" lineages in the Pampas and northern Patagonia. Therefore, we suggest early speciation in part of the *L. wiegmannii* complex might have been driven by the expansion of sand dunes throughout central Argentina and Pampas, in whose relicts, lineages A and B, and even *L. gardeli*, are now found. We further suggest that the ancestor of the northwestern lineages could have been restricted to sub-Andean mountains, where cyclic expansion and retraction of open habitats during climatic fluctuations would have favored diversification (Ortiz and Jayat, 2012 and references therein). Finally, the ancestor of the lowland arenicolous lineages (A & B) might have experimented subsequent speciation as a result of habitat fragmentation in more humid and warmer interglacial periods.

4.3. Taxonomic considerations

4.3.1. Nomenclatural considerations

The "South-Central Argentina" lineage has the broadest distribution of the complex, including the area of the type locality of *L. wiegmannii* in the surroundings of El Cóndor, near to the mouth of the Negro River in the Rio Negro Province of Argentina (Etheridge, 2000). Apparently, D'Orbigny and Gay collected specimens of *L. wiegmannii* in this area (along with *L. multimaculatus* and *Stenocercus pectinatus*) that were erroneously attributed to "Chile" in the original description of the species by Duméril and Bibron in 1837 (Etheridge, 2000). Moreover, from the perspective of *cytochrome b*, this lineage also occurs in the locality of Las Cañas in Uruguay, on the northern bank of the Negro River's mouth (Department of Río Negro, Uruguay); south of this river is the only known range of the "Uruguay" lineage. A similar pattern was also inferred for two mitochondrial haploclades of *Scapteromys* rodents (D'Elía and Pardiñas, 2004). The "Argentinean" lineage (*S. aquaticus*) is widely distributed between the Paraná and Uruguay Rivers also occurs in Las Cañas, Uruguay. As in *L. wiegmannii,* a second (*S. tumidus*) haploclade occurs further south of the Negro River's mouth, and is restricted to Uruguay and southeastern Rio Grande do Sul, Brazil. The concordance between these patterns suggests that the Uruguay River was a permeable geographic barrier at some point in the past, possibly during the Last Glacial Maximum (Iriondo, 1999; Tonni et al., 1999). If the candidate species inferred here are eventually diagnosed and described, the name *L. wiegmannii* should be reserved for those populations distributed in the south-central (and Atlantic coast) region of Argentina, and possibly, including also the population of Las Cañas (Río Negro, Uruguay). The latter population needs further genomic study to confirm its affinity to either to lineage A or B, or if both lineages co-occur at this locality.

4.3.2. Liolaemus gardeli

BPP strongly supported *Liolaemus gardeli* as a distinct lineage under all the scenarios explored, but sampling was based on four individuals only, which show almost no variation among them, and therefore this result should be taken with caution. In general, our analyses clearly show that *L. gardeli* comprises another lineage of the *Liolaemus wiegmannii* complex, closely related to Uruguay (B) and South-Central Argentinian (A) lineages. However, the phylogenetic relationships among these three lineages remain unresolved. For instance, when *L. gardeli* haplotypes are included in the *cytochrome b* tree, they group with LJAMM 13266 and 3132: two highly divergent haplotypes from the South-Central Argentina candidate species (A) (see Fig. S1). Increasing the number of individuals and inclusion of genomic data will be needed to adequately test the independence and phylogenetic position of *L. gardeli* within the complex.

Liolaemus gardeli is poorly differentiated morphologically from the other lineages of the complex (see Verrastro et al., 2017), which is again consistent with a very recent diversification. Issues of species boundaries and diagnoses for this and the other lineages of the *L. wiegmannii* complex warrant further study. Future studies should include genomic data for *L. gardeli* and a thorough study of morphological variation of the *L. wiegmannii* complex. This taxonomic clarification will also provide insight on whether the recent diversification of the complex represents complete speciation events or just the beginning of a

process that has generated "incipient" species (*sensu* Sukumaran and Knowles, 2017).

Acknowledgments

This work was funded by an ANII grant to AC (FCE_1_2014_1_104109), NSF-PIRE OISE (2005-2011) and CONICET and ANPCyT-FONCYT grants to MM (CONICET 5055/14, 2172/16, PIP 0336/13, 1397/11; PICT 1252/2015) and LJA (PIP 6469/04, PUE 0044/16, PICT 00506/06, 00784/11) and NSF award EF 1241885 to JWS. JV, AC and RM thank Pedeciba and SNI-ANII for additional financial support. JV is supported by a Doctoral scholarship of the graduate academic commission (CAP) of UdelaR, Uruguay. We thank J. Grummer, M. Golluchi and Grupo de Herpetología Patagónica members (C.H.F. Perez, M.M. Femenías, N. Frutos) for help collecting specimens. J. Grummer provided valuable advice for improving DNA extraction quality. This research used the computational resources of ClusterUY: www.cluster.uy.

Data Accessibility

Sequence data are available through GenBank accession numbers: MK814191-MK814341 (CYTB); MK825649-MK825732 (KIF24); MK825610-MK825648 (PRLR); MK825592-MK825609 (EXPH5).

Declaration of Competing Interest

We the authors declare no competing interests.

Appendix A. Bayes Factor species delimitation results for the *Liolaemus wiegmannii* complex using a 595 SNPs matrix that allows 5% of missing data. Model 1 represents the most speciose scenario where each group from the DAPC represent a distinct candidate species. Subsequent models derive from lumping some of these lineages. A: South-Central Argentina; B: Uruguay; D: Catamarca; E: Tucumán-Salta i; F: Jujuy; G: Salta II. Models numbered here are not necessarily equivalent to the ones presented in Table 3.

Model	Species	Retained SNPs	Marginal Likelihood	Rank	$2log_eBF$
1	6: A, B, D, E, F, G	325	−2097.03	1	–
2	5: A, B, D, E, FG	406	−2618.98	2	+1043.90
3	4: AB, D, E, FG	412	−2741.41	3	+1288.76
4	3: AB, D, EFG	483	−3241.61	5	+2289.18
5	4: A, B, D, EFG	477	−3111.98	4	+2029.92
6	2: AB, DEFG	595	−4351.16	6	+4508.27
7	2: ABD, EFG	584	−5258.49	7	+6322.94

Appendix B. Supplementary material

Supplementary data to this article can be found online at https://doi.org/10.1016/j.ympev.2019.05.024.

References

Abdala, C.S., Quinteros, A.S., 2014. Los últimos 30 años de estudios de la familia de lagartijas más diversa de Argentina. Cuad. Herpetol. 28 (2), 55–82.

Agapow, P.M., Bininda-Emonds, O.R., Crandall, K.A., Gittleman, J.L., Mace, G.M., Marshall, J.C., Purvis, A., 2004. The impact of species concept on biodiversity studies. Q. Rev. Biol 79 (2), 161–179.

Avila, L.J., 2003. A new species of *Liolaemus* (Squamata: Liolaemidae) from northeastern Argentina and southern Paraguay. Herpetologica 59 (2), 283–292.

Avila, L.J., Morando, M., Sites, J.W., 2006. Congeneric phylogeography: hypothesizing species limits and evolutionary processes in Patagonian lizards of the *Liolaemus boulengeri* group (Squamata: Liolaemini). Biol. J. Linnean. Soc. 89 (2), 241–275. https://doi.org/10.1111/j.1095-8312.2006.00666.x.

Avila, L.J., Morando, M., Perez, D.R., Sites Jr, J.W., 2009. A new species of *Liolaemus* from Añelo sand dunes, northern Patagonia, Neuquén, Argentina, and molecular phylogenetic relationships of the *Liolaemus wiegmannii* species group (Squamata, Iguania, Liolaemini). Zootaxa 2234, 39–55.

Avila, L.J., Perez, C.H.F., Medina, C.D., Sites Jr, J.W., Morando, M., 2012. A new species of lizard of the *Liolaemus elongatus* clade (Reptilia: Iguania: Liolaemini) from Curi Leuvu River Valley, northern Patagonia, Neuquen Argentina. Zootaxa 3325 (1), 37–52.

Avila, L.J., Martínez, L.E., Morando, M., 2013. Checklist of lizards and amphisbaenians of Argentina: an update. Zootaxa 3616, 201–238. https://doi.org/10.11646/zootaxa.3616.3.1.

Avila, L.J., Medina, C.D., Perez, C.H.F., Sites Jr, J.W., Morando, M., 2015. Molecular phylogenetic relationships of the lizard clade *Liolaemus elongatus* (Iguania: Liolaemini) with the description of a new species from an isolated volcanic peak in northern Patagonia. Zootaxa 3947 (1), 067–084. https://doi.org/10.11646/zootaxa.3947.1.4.

Avila, L.J., Perez, C.H.F., Minoli, I., Medina, C.D., Sites, J.W., Morando, M., 2017. New species of *Liolaemus* (Reptilia, Squamata, Liolaemini) of the Liolaemus donosobarrosi clade from northwestern Patagonia, Neuquén province Argentina. Zootaxa 4362 (4), 535–563. https://doi.org/10.11646/zootaxa.4362.4.4.

Battey, C.J., Klicka, J., 2017. Cryptic speciation and gene flow in a migratory songbird species complex: insights from the red-eyed vireo (*Vireo olivaceus*). Mol. Phylogenet. Evol. 113, 67–75. https://doi.org/10.1016/j.ympev.2017.05.006.

Bauer, A.M., Parham, J.F., Brown, R.M., Stuart, B.L., Grismer, L., Papenfuss, T.J., Bohme, W., Savage, J.M., Carranza, S., Grismer, J.L., Wagner, P., Schmitz, A., Ananjeva, N.B., Inger, R.F., 2011. Availability of new Bayesian-delimited gecko names and the importance of character-based species descriptions. Proc. R. Soc. Lond. B Biol. Sci. 278, 490–492. https://doi.org/10.1098/rspb.2010.1330.

Bickford, D., Lohman, D.J., Sodhi, N.S., Ng, P.K., Meier, R., Winker, K., Ingram, K.K., Das, I., 2007. Cryptic species as a window on diversity and conservation. Trends Ecol. Evol. 22 (3), 148–155. https://doi.org/10.1016/j.tree.2006.11.004.

Bouckaert, R., Heled, J., Kühnert, D., Vaughan, T., Wu, C.-H., Xie, D., Suchard, M.A., Rambaut, A., Drummond, A.J., 2014. BEAST 2: a software platform for bayesian evolutionary analysis. PLoS Comput. Biol. 10 (4), e1003537. https://doi.org/10.1371/journal.pcbi.1003537.

Breitman, M.F., Avila, L.J., Sites Jr, J.W., Morando, M., 2011a. Lizards from the end of the world: phylogenetic relationships of the *Liolaemus lineomaculatus* section (Squamata: Iguania: Liolaemini). Mol. Phylogenet. Evol. 59 (2), 364–376. https://doi.org/10.1016/j.ympev.2011.02.008.

Breitman, M.F., Pérez, C.H.F., Parra, M., Morando, M., Sites Jr., J.W., Avila, L.J., 2011b. New species of lizard from the magellanicus clade of the *Liolaemus lineomaculatus* section (Squamata: Iguania: Liolaemidae) from southern Patagonia. Zootaxa 3123, 32–48.

Breitman, M.F., Parra, M., Pérez, C.H.F., Sites Jr, J.W., 2011c. Two new species of lizards from the *Liolaemus lineomaculatus* section (Squamata: Iguania: Liolaemidae) from southern Patagonia. Zootaxa 3120 (1), 01–28.

Breitman, M.F., Avila, L.J., Sites, J.W., Morando, M., 2012. How lizards survived blizzards: phylogeography of the *Liolaemus lineomaculatus* group (Liolaemidae) reveals multiple breaks and refugia in southern Patagonia and their concordance with other codistributed taxa. Mol. Ecol. 21 (24), 6068–6085. https://doi.org/10.1111/mec.12075.

Bryant, D., Bouckaert, R., Felsenstein, J., Rosenberg, N.A., RoyChoudhury, A., 2012. Inferring species trees directly from biallelic genetic markers: bypassing gene trees in a full coalescent analysis. Mol. Phylogenet. Evol. 29 (8), 1917–1932. https://doi.org/10.1093/molbev/mss086.

Cabrera, M.P., Scrocchi, G.J., Cruz, F.B., 2013. Sexual size dimorphism and allometry in *Liolaemus* of the *L. laurenti* group (Sauria: Liolaemidae): Morphologic lability in a clade of lizards with different reproductive modes. Zool. Anz. 252 (3), 299–306. https://doi.org/10.1016/j.jcz.2012.08.003.

Camargo, A., Sinervo, B., Sites Jr, J.W., 2010. Lizards as model organisms for linking phylogeographic and speciation studies. Mol. Ecol. 19 (16), 3250–3270. https://doi.org/10.1111/j.1365-294X.2010.04722.x.

Catchen, J., Hohenlohe, P.A., Bassham, S., Amores, A., Cresko, W.A., 2013. Stacks: an analysis tool set for population genomics. Mol. Ecol. 22 (11), 3124–3140. https://doi.org/10.1111/mec.12354.

Chifman, J., Kubatko, L., 2014. Quartet inference from SNP data under the coalescent

model. Bioinformatics 30 (23), 3317–3324. https://doi.org/10.1093/bioinformatics/btu530.
Corl, A., Davis, A.R., Kuchta, S.R., Comendant, T., Sinervo, B., 2010. Alternative mating strategies and the evolution of sexual size dimorphism in the side-blotched lizard, *Uta stansburiana*: a population-level comparative analysis. Evolution 64 (1), 79–96. https://doi.org/10.1111/j.1558-5646.2009.00791.x.
Darriba, D., Taboada, G.L., Doallo, R., Posada, D., 2012. jModelTest 2: more models, new heuristics and parallel computing. Nat. Methods 9, 772. https://doi.org/10.1038/nmeth.2109.
D'Elía, G., Pardiñas, U.F., 2004. Systematics of argentinean, paraguayan, and uruguayan swamp rats of the genus *Scapteromys* (Rodentia, Cricetidae, Sigmodontinae). J. Mammal. 85 (5), 897–910. https://doi.org/10.1644/BRB-201.
Díaz-Arce, N., Arrizabalaga, H., Murua, H., Irigoien, X., Rodríguez-Ezpeleta, N., 2016. RAD-seq derived genome-wide nuclear markers resolve the phylogeny of tunas. Mol. Phylogenet. Evol. 102, 202–207. https://doi.org/10.1016/j.ympev.2016.06.002.
Drummond, A.J., Rambaut, A., 2007. BEAST: Bayesian evolutionary analysis by sampling trees. BMC Evol. Biol. 7, 214. https://doi.org/10.1186/1471-2148-7-214.
Drummond, A.J., Suchard, M.A., Xie, D., Rambaut, A., 2012. Bayesian phylogenetics with BEAUti and the BEAST 1.7. Mol. Biol. Evol. 29, 1969–1973. https://doi.org/10.1093/molbev/mss075.
Etheridge, R.E., 1995. Redescription of *Ctenoblepharys adspersa* Tschudi, 1845, and the taxonomy of Liolaeminae (Reptilia: Squamata: Tropiduridae). Am. Mus. Novit. 3142, 1–34.
Etheridge, R., 2000. A review of lizards of the *Liolaemus wiegmannii* group (Squamata, Iguania, Tropiduridae), and a history of morphological change in the sand-dwelling species. Herpetol. Monogr. 14, 293–352.
Filatov, D.A., 2009. Processing and population genetic analysis of multigenic datasets with ProSeq3 software. Bioinformatics 25, 3189–3190. https://doi.org/10.1093/bioinformatics/btp572.
Fontanella, F.M., Olave, M., Avila, L.J., Sites, J.W., Morando, M., 2012. Molecular dating and diversification of the South American lizard genus *Liolaemus* (subgenus Eulaemus) based on nuclear and mitochondrial DNA sequences. Zool. J. Linnean Soc. 164 (4), 825–835. https://doi.org/10.1111/j.1096-3642.2011.00786.x.
Fujita, M.K., Leaché, A.D., 2011. A coalescent perspective on delimiting and naming species: a reply to Bauer et al. Proc. R. Soc. B. 278 (1705), 493–495. https://doi.org/10.1098/rspb.2010.1864.
Fujita, M.K., Leaché, A.D., Burbrink, F.T., McGuire, J.A., Moritz, C., 2012. Coalescent-based species delimitation in an integrative taxonomy. Trends Ecol. Evol. 27 (9), 480–488. https://doi.org/10.1016/j.tree.2012.04.012.
Gibbs, H.L., Sovic, M., Amazonas, D., Chalkidis, H., Salazar-Valenzuela, D., Moura-Da-Silva, A.M., 2018. Recent lineage diversification in a venomous snake through dispersal across the Amazon River. Biol. J. Linn. Soc. 123 (3), 651–665. https://doi.org/10.1093/biolinnean/blx158.
Gordon, A., Hannon, G.J. 2010. Fastx-toolkit. FASTQ/A short-reads preprocessing tools (unpublished). http://hannonlab.cshl.edu/fastx_toolkit/.
Grummer, J.A., Bryson, R.W., Reeder, T.W., 2014. Species delimitation using Bayes factors: simulations and application to the *Sceloporus scalaris* species group (Squamata: Phrynosomatidae). Syst. Biol. 63 (2), 119–133. https://doi.org/10.1093/sysbio/syt069.
Heled, J., Drummond, A.J., 2010. Bayesian inference of species trees from multilocus data. Mol. Biol. Evol. 27 (3), 570–580. https://doi.org/10.1093/molbev/msp274.
Herrera, S., Shank, T.M., 2016. RAD sequencing enables unprecedented phylogenetic resolution and objective species delimitation in recalcitrant divergent taxa. Mol. Phylogenet. Evol. 100, 70–79. https://doi.org/10.1016/j.ympev.2016.03.010.
Helyar, S.J., Hemmer-Hansen, J., Bekkevold, D., Taylor, M.I., Ogden, R., Limborg, M.T., Cariani, A., Maes, G.E., Diopere, E., Carvalho, G.R., Nielsen, E.E., 2011. Application of SNPs for population genetics of non-model organisms: new opportunities and challenges. Mol. Ecol. Resour. 11, 123–136. https://doi.org/10.1111/j.1755-0998.2010.02943.x.
Hoelzer, G.A., Meinick, D.J., 1994. Patterns of speciation and limits to phylogenetic resolution. Trends Ecol. Evol. 9 (3), 104–107. https://doi.org/10.1016/0169-5347(94)90207-0.
Hudson, R.R., Coyne, J.A., 2002. Mathematical consequences of the genealogical species concept. Evolution 56 (8), 1557–1565. https://doi.org/10.1111/j.0014-3820.2002.tb01467.x.
Hung, C.M., Drovetski, S.V., Zink, R.M., 2016. Matching loci surveyed to questions asked in phylogeography. Proc. R. Soc. B 283 (1826), 20152340. https://doi.org/10.1098/rspb.2015.2340.
Iriondo, M., 1999. Climatic changes in the South American plains: records of a continent-scale oscillation. Quat. Int. 57, 93–112. https://doi.org/10.1016/S1040-6182(98)00053-6.
Jombart, T., 2008. adegenet: a R package for the multivariate analysis of genetic markers. Bioinformatics 24 (11), 1403–1405. https://doi.org/10.1093/bioinformatics/btn129.
Kapli, P., Lutteropp, S., Zhang, J., Kobert, K., Pavlidis, P., Stamatakis, A., Flouri, T., 2017. Multi-rate Poisson tree processes for single-locus species delimitation under maximum likelihood and Markov chain Monte Carlo. Bioinformatics 33 (11), 1630–1638. https://doi.org/10.1093/bioinformatics/btx025.
Kass, R.E., Raftery, A.E., 1995. Bayes factors. J. Am. Stat. Assoc. 90, 773–795.
Kozlov, A., Darriba, D., Flouri, T., Morel, B., Stamatakis, A., 2018. RAxML-NG: A fast, scalable, and user-friendly tool for maximum likelihood phylogenetic inference. bioRxiv 447110. https://doi.org/10.1101/447110.
Larkin, M.A., Blackshields, G., Brown, N.P., Chenna, R., McGettigan, P.A., McWilliam, H., Valentin, F., Wallace, I.M., Wilm, A., Lopez, R., Thompson, J.D., Gibson, T.J., Higgins, D.G., 2007. Clustal W and clustal X version 2.0. Bioinformatics 23 (21), 2947–2948. https://doi.org/10.1093/bioinformatics/btm404.
Leaché, A.D., Fujita, M.K., 2010. Bayesian species delimitation in West African forest geckos (*Hemidactylus fasciatus*). Proc. R. Soc. B. 277 (1697), 3071–3077. https://doi.org/10.1098/rspb.2010.0662.
Leaché, A.D., Fujita, M.K., Minin, V.N., Bouckaert, R.R., 2014. Species delimitation using genome-wide SNP data. Syst. Biol. 63 (4), 534–542. https://doi.org/10.1093/sysbio/syu018.
Leaché, A.D., Oaks, J.R., 2017. The utility of single nucleotide polymorphism (SNP) data in phylogenetics. Annu. Rev. Ecol. Evol. Syst. 48, 69–84. https://doi.org/10.1146/annurev-ecolsys-110316-022645.
Leaché, A.D., McElroy, M.T., Trinh, A., 2018. A genomic evaluation of taxonomic trends through time in coast horned lizards (genus *Phrynosoma*). Mol. Ecol. 27, 2884–2895. https://doi.org/10.1111/mec.14715.
Leaché, A.D., Zhu, T., Rannala, B., Yang, Z., 2019. The spectre of too many species. Syst. Biol. 68, 168–181. https://doi.org/10.1093/sysbio/syy051.
Lee, K.M., Kivelä, S.M., Ivanov, V., Hausmann, A., Kaila, L., Wahlberg, N., Mutanen, M., 2018. Information dropout patterns in restriction site associated DNA phylogenomics and a comparison with multilocus Sanger data in a species-rich moth genus. Syst. Biol. 67, 925–939. https://doi.org/10.1093/sysbio/syy029.
Lobo, F., Espinoza, R.E., Quinteros, S., 2010. A critical review and systematic discussion of recent classification proposals for liolaemid lizards. Zootaxa 2549, 1–30.
Maddison, W.P., 1997. Gene trees in species trees. Syst. Biol. 46 (3), 523–536. https://doi.org/10.1093/sysbio/46.3.523.
Martinez, L.E., Avila, L.J., Pérez, C.H.F., Perez, D.R., Sites Jr, J.W., Morando, M., 2011. A new species of *Liolaemus* (Squamata, Iguania, Liolaemini) endemic to the Auca Mahuida volcano, northwestern Patagonia, Argentina. Zootaxa 3010 (1), 31–46.
Medina, C.D., Avila, L.J., Sites Jr, J.W., Morando, M., 2015. Molecular phylogeny of the *Liolaemus kriegi* complex (Iguania, Liolaemini). Herpetologica 71 (2), 143–151. https://doi.org/10.1655/HERPETOLOGICA-D-13-00083.
Medina, C.D., Avila, L.J., Sites Jr, J.W., Morando, M., 2017. Phylogeographic history of Patagonian lizards of the *Liolaemus elongatus* complex (Iguania: Liolaemini) based on mitochondrial and nuclear DNA sequences. J. Zool. Syst. Evol. Res. 55 (3), 238–249. https://doi.org/10.1111/jzs.12163.
Morando, M., Avila, L.J., Sites Jr, J.W., 2003. Sampling strategies for delimiting species: genes, individuals, and populations in the *Liolaemus elongatus-kriegi* complex (Squamata: Liolaemidae) in Andean-Patagonian South America. Syst. Biol. 52 (2), 159–185. https://doi.org/10.1080/10635150390192717.
Morando, M., Avila, L.J., Baker, J., Sites Jr, J.W., 2004. Phylogeny and phylogeography of the *Liolaemus darwinii* complex (Squamata: Liolaemidae): evidence for introgression and incomplete lineage sorting. Evolution 58 (4), 842–859. https://doi.org/10.1111/j.0014-3820.2004.tb00416.x.
Morando, M., Avila, L.J., Turner, C.R., Sites Jr, J.W., 2007. Molecular evidence for a species complex in the patagonian lizard *Liolaemus bibronii* and phylogeography of the closely related *Liolaemus gracilis* (Squamata: Liolaemini). Mol. Phylogenet. Evol. 43 (3), 952–973. https://doi.org/10.1016/j.ympev.2006.09.012.
Morin, P.A., Luikart, G., Wayne, R.K., 2004. SNPs in ecology, evolution and conservation. Trends Ecol. Evol. 19 (4), 208–216. https://doi.org/10.1016/j.tree.2004.01.009.
Nei, M., 1987. Molecular evolutionary genetics. Columbia University Press, New York, pp. 1–512.
Nieto-Montes de Oca, A., Barley, A.J., Meza-Lázaro, R.N., García-Vázquez, U.O., Zamora-Abrego, J.G., Thomson, R.C., Leaché, A.D., 2017. Phylogenomics and species delimitation in the knob-scaled lizards of the genus *Xenosaurus* (Squamata: Xenosauridae) using ddRADseq data reveal a substantial underestimation of diversity. Mol. Phylogenet. Evol. 106, 241–253. https://doi.org/10.1016/j.ympev.2016.09.001.
Noguerales, V., Cordero, P.J., Ortego, J., 2018. Integrating genomic and phenotypic data to evaluate alternative phylogenetic and species delimitation hypotheses in a recent evolutionary radiation of grasshoppers. Mol. Ecol. 27 (5), 1229–1244. https://doi.org/10.1111/mec.14504.
Noonan, B.P., Yoder, A.D., 2009. Anonymous nuclear markers for Malagasy plated lizards (*Zonosaurus*). Mol. Ecol. Resour. 9 (1), 402–404. https://doi.org/10.1111/j.1755-0998.2008.02250.x.
Oaks, J.R., Cobb, K.A., Minin, V.N., Leaché, A.D., 2019. Marginal likelihoods in phylogenetics: a review of methods and applications. Syst. Biol. https://doi.org/10.1093/sysbio/syz003.
O'Connell, K.A., Smith, E.N., Shaney, K.J., Arifin, U., Kurniawan, N., Sidik, I., Fujita, M.K., 2018. Coalescent species delimitation of a Sumatran parachuting frog. Zool. Scr. 47 (1), 33–43. https://doi.org/10.1111/zsc.12248.
O'Connell, K.A., Smith, E.N., 2018. The effect of missing data on coalescent species delimitation and a taxonomic revision of whipsnakes (Colubridae: *Masticophis*). Mol. Phylogenet. Evol. 127, 356–366. https://doi.org/10.1016/j.ympev.2018.03.018.
Olave, M., Avila, L.J., Sites, J.W., Morando, M., 2014. Multilocus phylogeny of the widely distributed South American lizard clade *Eulaemus* (Liolaemini, *Liolaemus*). Zool. Scr. 43 (4), 323–337. https://doi.org/10.1111/zsc.12053.
Olave, M., Avila, L.J., Sites, J.W., Morando, M., 2015. Model-based approach to test hard polytomies in the *Eulaemus* clade of the most diverse South American lizard genus *Liolaemus* (Liolaemini, Squamata). Zool. J. Linnean Soc. 174 (1), 169–184. https://doi.org/10.1111/zoj.12231.
Olave, M., Avila, L.J., Sites Jr, J.W., Morando, M., 2017. Hidden diversity within the lizard genus *Liolaemus*: genetic vs morphological divergence in the *L. rothi* complex (Squamata: Liolaeminae). Mol. Phylogenet. Evol. 107, 56–63. https://doi.org/10.1016/j.ympev.2016.09.009.
Ortiz, P.E., Jayat, J.P., 2012. The Quaternary record of *Reithrodon auritus* (Rodentia: Cricetidae) in northwestern Argentina and its paleoenvironmental meaning. Mammalia 76 (4), 455–460. https://doi.org/10.1515/mammalia-2012-0059.
Palumbi, S.R., 1996. Nucleic acids II: the polymerase chain reaction. In: Hillis, D.M., Mable, B.K., Moritz, C. (Eds.), Molecular Systematics. Sinauer Associates, Sunderland, pp. 205–247.

Pante, E., Puillandre, N., Viricel, A., Arnaud-Haond, S., Aurelle, D., Castelin, M., Chenuil, A., Destombe, C., Forcioli, D., Valero, M., Viard, F., Samadi, S., 2015a. Species are hypotheses: avoid connectivity assessments based on pillars of sand. Mol. Ecol. 24 (3), 525–544. https://doi.org/10.1111/mec.13048.

Pante, E., Abdelkrim, J., Viricel, A., Gey, D., France, S.C., Boisselier, M.C., Samadi, S., 2015b. Use of RAD sequencing for delimiting species. Heredity 114 (5), 450–459. https://doi.org/10.1038/hdy.2014.105.

Peterson, B.K., Weber, J.N., Kay, E.H., Fisher, H.S., Hoekstra, H.E., 2012. Double digest RADseq: an inexpensive method for de novo SNP discovery and genotyping in model and non-model species. PloS One 7 (5), e37135. https://doi.org/10.1371/journal.pone.0037135.

Pfenninger, M., Schwenk, K., 2007. Cryptic animal species are homogeneously distributed among taxa and biogeographical regions. BMC Evol. Biol. 7 (1), 121. https://doi.org/10.1186/1471-2148-7-121.

Pincheira-Donoso, D., Scolaro, J.A., Sura, P., 2008. A monographic catalogue on the systematics and phylogeny of the South American iguanian lizard family Liolaemidae (Squamata, Iguania). Zootaxa 1800, 1–85.

Pons, J., Barraclough, T.G., Gomez-Zurita, J., Cardoso, A., Duran, D.P., Hazell, S., Kamoun, S., Sumlin, W.D., Vogler, A.P., 2006. Sequence-based species delimitation for the DNA taxonomy of undescribed insects. Syst. Biol. 55 (4), 595–609. https://doi.org/10.1080/10635150600852011.

Portik, D.M., Wood Jr, P.L., Grismer, J.L., Stanley, E.L., Jackman, T.R., 2012. Identification of 104 rapidly-evolving nuclear protein-coding markers for amplification across scaled reptiles using genomic resources. Conserv. Genet. Resour. 4 (1), 1–10. https://doi.org/10.1007/s12686-011-9460-1.

R Core Team, 2018. R: A language and environment for statistical computing. R Foundation for Statistical Computing, Vienna, Austria.

Rabassa, J., Coronato, A.M., Salemme, M., 2005. Chronology of the Late Cenozoic Patagonian glaciations and their correlation with biostratigraphic units of the Pampean region (Argentina). J. S. Am. Earth. Sci. 20 (1), 81–103. https://doi.org/10.1016/j.jsames.2005.07.004.

Rambaut, A., Drummond, A., 2007. Tracer v1.6. Available at: http://tree.bio.ed.ac.uk/software/tracer.

Rannala, B., Yang, Z., 2003. Bayes estimation of species divergence times and ancestral population sizes using DNA sequences from multiple loci. Genetics 164 (4), 1645–1656.

Reyes-Velasco, J., Mulcahy, D.G., 2010. Additional taxonomic remarks on the genus *Pseudoleptodeira* (Serpentes: Colubridae) and the phylogenetic placement of "*P. uribei*". Herpetologica 66 (1), 99–110. https://doi.org/10.1655/09-019.1.

Rokas, A., Krüger, D., Carroll, S.B., 2005. Animal evolution and the molecular signature of radiations compressed in time. Science 310 (5756), 1933–1938. https://doi.org/10.1126/science.1116759.

Rozas, J., Rozas, R., 1995. DnaSP, DNA sequence polymorphism: an interactive program for estimating Population Genetics parameters from DNA sequence data. Comput. Appl. Biosci. 11, 621–625. https://doi.org/10.1093/bioinformatics/11.6.621.

Ruane, S., Bryson Jr, R.W., Pyron, R.A., Burbrink, F.T., 2014. Coalescent species delimitation in milksnakes (genus Lampropeltis) and impacts on phylogenetic comparative analyses. Syst. Biol. 63 (2), 231–250.

Schliep, K.P., 2011. phangorn: phylogenetic analysis in R. Bioinformatics 27 (4), 592. https://doi.org/10.1093/bioinformatics/btq706.

Schulte, J.A., Macey, J.R., Espinoza, R.E., Larson, A., 2000. Phylogenetic relationships in the iguanid lizard genus *Liolaemus*: multiple origins of viviparous reproduction and evidence for recurring Andean vicariance and dispersal. Biol. J. Linnean Soc. 69 (1), 75–102. https://doi.org/10.1111/j.1095-8312.2000.tb01670.x.

Soibelzon, E., Tonni, E.P., 2009. Early Pleistocene glaciations in Argentina (South America) and the response of the mammals: the case of the Pampean Region. Curr. Res. Pleistoc. 26, 175–177.

Stamatakis, A., 2014. RAxML version 8: a tool for phylogenetic analysis and post-analysis of large phylogenies. Bioinformatics 30 (9), 1312–1313. https://doi.org/10.1093/bioinformatics/btu033.

Stellatelli, O.A., Bo, M.S., Madrid, E., Vega, L.E., Block, C., 2014. Nueva localidad para *Liolaemus wiegmannii* (Duméril & Bibrón, 1837) en la Provincia de Río Negro (Argentina). Cuad. Herpetol. 28 (1), 51–52.

Struck, T.H., Feder, J.L., Bendiksby, M., Birkeland, S., Cerca, J., Gusarov, V.I., Kistenich, S., Larsson, K.H., Liow, L.H., Nowak, M.D., Stedje, B., Bachmann, L., Dimitrov, D., 2018. Finding evolutionary processes hidden in cryptic species. Trends Ecol. Evol. 33 (3), 153–163. https://doi.org/10.1016/j.tree.2017.11.007.

Sukumaran, J., Knowles, L.L., 2017. Multispecies coalescent delimits structure, not species. Proc. Natl. Acad. Sci. 114 (7), 1607–1612. https://doi.org/10.1073/pnas.1607921114.

Swofford, D.L., 1998. Paup 4.0 Beta Version for Windows: Phylogenetic analysis using parsimony. Sinauer Associates, Sunderland.

Tamura, K., Stecher, G., Peterson, D., Filipski, A., Kumar, S., 2013. MEGA6: molecular evolutionary genetics analysis version 6.0. Mol. Biol. Evol. 30, 2725–2729. https://doi.org/10.1093/molbev/mst197.

Tonni, E.P., Cione, A.L., Figini, A.J., 1999. Predominance of arid climates indicated by mammals in the pampas of Argentina during the Late Pleistocene and Holocene. Palaeogeogr. Palaeoclimatol. Palaeoecol. 147 (3), 257–281. https://doi.org/10.1016/S0031-0182(98)00140-0.

Townsend, T.M., Alegre, R.E., Kelley, S.T., Wiens, J.J., Reeder, T.W., 2008. Rapid development of multiple nuclear loci for phylogenetic analysis using genomic resources: an example from squamate reptiles. Mol. Phylogenet. Evol. 47 (1), 129–142. https://doi.org/10.1016/j.ympev.2008.01.008.

Troncoso-Palacios, J., Diaz, H.A., Puas, G.I., Riveros-Riffo, E., Elorza, A.A., 2016. Two new *Liolaemus* lizards from the Andean highlands of southern Chile (Squamata, Iguania, Liolaemidae). ZooKeys 632, 121–146. https://doi.org/10.3897/zookeys.632.9528.

Uetz, P., 2019. The Reptile Database. accessed February 28, 2019. http://www.reptile-database.org.

Vega, L.E., Quinteros, A.S., Stellatelli, O.A., Bellagamba, P.J., Block, C., Madrid, E.A., 2018. A new species of the *Liolaemus alticolor-bibronii* group (Iguania: Liolaemidae) from East-central Argentina. Zootaxa 4379 (4), 539–555. https://doi.org/10.11646/zootaxa.4379.4.6.

Verrastro, L., Veronese, L., Bujes, C., Dias Filho, M.M., 2003. A new species of *Liolaemus* from southern Brazil (Iguania: Tropiduridae). Herpetologica 59 (1), 105–118. https://doi.org/10.1655/0018-0831(2003) 059[0105:ANSOLF]2.0.CO;2.

Verrastro, L., Maneyro, R., Da Silva, C.M., Farias, I., 2017. A new species of lizard of the *L. wiegmannii* group (Iguania: Liolaemidae) from the Uruguayan Savanna. Zootaxa 4294 (4), 443–461.

Villamil, J., Camargo, A., Maneyro, R., 2017. Morphological variation and sexual dimorphism in *Liolaemus wiegmannii* (Duméril & Bibron, 1837)(Squamata: Liolaemidae) from Uruguay. Acta Herpetol. 12 (1), 3–17. https://doi.org/10.13128/Acta_Herpetol-18188.

Wagner, C.E., Keller, I., Wittwer, S., Selz, O.M., Mwaiko, S., Greuter, L., Silvasunder, A., Seehausen, O., 2013. Genome-wide RAD sequence data provide unprecedented resolution of species boundaries and relationships in the Lake Victoria cichlid adaptive radiation. Mol. Ecol. 22 (3), 787–798. https://doi.org/10.1111/mec.12023.

Wang, X., Ye, X., Zhao, L., Li, D., Guo, Z., Zhuang, H., 2017. Genome-wide RAD sequencing data provide unprecedented resolution of the phylogeny of temperate bamboos (Poaceae: Bambusoideae). Sci. Rep. 7 (1), 11546. https://doi.org/10.1038/s41598-017-11367-x.

Yang, Z., Rannala, B., 2010. Bayesian species delimitation using multilocus sequence data. Proc. Nat. Acad. Sci. 107 (20), 9264–9269. https://doi.org/10.1073/pnas.0913022107.

Yang, Z., Rannala, B., 2014. Unguided species delimitation using DNA sequence data from multiple loci. Mol. Biol. Evol 31 (12), 3125–3135. https://doi.org/10.1093/molbev/msu279.

Yang, Z., 2015. The BPP program for species tree estimation and species delimitation. Curr. Zool. 61 (5), 854–865. https://doi.org/10.1093/czoolo/61.5.854.

Zhang, C., Zhang, D.X., Zhu, T., Yang, Z., 2011. Evaluation of a Bayesian coalescent method of species delimitation. Syst. Biol. 60 (6), 747–761. https://doi.org/10.1093/sysbio/syr071.